DEVELOPMENT AND VALIDATION OF A COLORIMETRIC PROBE FOR DETECTION OF BACTERIAL WILT OF TOMATO IN KENYA

IVY LYNN AOKO OPIYO

MASTER OF SCIENCE

(Horticulture)

JOMO KENYATTA UNIVERSITY

OF

AGRICULTURE AND TECHNOLOGY

2022

Development and Validation of a Colorimetric Probe for Detection of Bacterial Wilt of Tomato in Kenya

Ivy Lynn Aoko Opiyo

A Thesis Submitted in Partial Fulfillment of the Requirements for the Degree of Master of Science in Horticulture of the Jomo Kenyatta University of Agriculture and Technology

2022

DECLARATION

This thesis is my original work and has not been presented for a degree at any other University.

Signature……..…….…. Date……

Ivy Lynn Aoko Opiyo

This thesis has been submitted for examination with our approval as University Supervisors.

Signature……..…….…. Date……

Dr. Agnes Kavoo, PhD

JKUAT, Kenya

Signature……..…….…. Date……

Dr. Dezzline Ondigo, PhD

Kar.U, Kenya

Signature……..…….…. Date……

Dr. Cornelius Wainaina, PhD

JKUAT, Kenya

DEDICATION

To my beloved mother and father for their unending love, support and encouragement.

ACKNOWLEDGEMENTS

I want to thank the Almighty God for his eternal grace that has enabled the completion of this thesis. A very special mention goes to my supervisors, Dr. Agnes Kavoo, Dr.Dezzline Ondigo and Dr. Cornelius Wainaina, for their immense patience, guidance, availability and support throughout this entire journey. A special thank you goes to Africa-ai-Japan, who funded the research work. I extend my sincere gratitude to Jomo Kenyatta University of Agriculture and Technology for allowing us to conduct research and publish my work. I am also much grateful to Dr. Leonard Kiirika and Dr. Mwashasha Mwajita for their mentorship. Many thanks to all the Horticulture and Chemistry department laboratory technicians and postgraduate students for their support and encouragement. To all the farmers in Kajiado, Kirinyanga, Bomet and Kiambu who allowed me to visit and collect samples from their farms, you made this possible.

To my incredible family, thank you (especially my mother for her prayers, moral and financial support) for your endless support, understanding and unconditional love, be blessed.\

TABLE OF CONTENTS

LIST OF TABLES

LIST OF FIGURES

LIST OF ABBREVIATIONS/ACRONYMS

AuNPs	Gold Nanoparticles
CPG	Casamino acid Peptone-Glucose
DLS	Dynamic Light Scattering
DNA	Deoxyribonucleic acid
ELISA	Enzyme-linked Immunosorbent Assay
E. U	European Union
FAO	Food and Agricultural Organisation
FISH	Fluorescence in situ hybridization
FT-IR	Fourier transform infrared spectroscopy
GA	Gibberellic acid
GDP	Gross domestic product
NPs	Nano particles
PCR	Polymerase Chain Reaction
RNA	Ribonucleic acid
SEM	Scanning Electron Microscopy
SPR	Surface Plasmon Resonance
TEM	Transmission Electron Microscopy
TZC	Tetrazolium chloride

ABSTRACT

Kenya is ranked 6th among the African countries leading in tomato production, with approximately 14% of total vegetable production and 6.72% of horticultural crops. Despite its importance, tomato production is threatened by a wide range of diseases and pests, which result in up to 42% yield losses. Bacterial wilt disease caused by *Ralstonia solanacearum*. a soil-borne pathogen is a severe threat to the production of over 400 plant species, particularly crops in the Solanaceae family, including tomato and potato. Crop losses can be reduced, and specific treatments developed to control the pathogen if the disease is accurately diagnosed and identified prior to spreading. Existing bacterial wilt identification and detection methods present a wide range of limitations in their use. These conventional methods employ many techniques that involve extensive sample preparation steps before analysis, making them a potential source of error. They are also expensive, time-consuming, and require skilled labour to utilize, thus limiting the effectiveness of any remedial strategy. A rapid, efficient, and user-friendly detection method for most host crops is still lacking. This necessitates the development of methods that are; simple, selective and capable of being used by non-skilled persons in the field. Colorimetric probes can overcome the challenges presented by most conventional detection methods since signaling of the targeted event can be visualized in real-time by the "naked eye". This study presents the development of a gold-nanoparticle-based colorimetric probe to detect *Ralstonia solanacearum* through gibberellic acid exudation signalling event. The objectives of this study were to develop a diagnostic probe using gold nanoparticles, quantify the gibberellins produced during *Ralstonia*-tomato interaction and validate the efficacy of the designed probe under *in-vitro* conditions. The gold nanoparticles (AuNPs) were chemically synthesized through reduction with citrate ion and characterized using Transmission electron microscopy (TEM) and Dynamic light scattering (DLS) to determine their size. The optical properties of AuNPs solution and its interaction with Gibberellic acid (GA) secreted by *Ralstonia Solanacearum* was evaluated using Uv-vis spectrophotometry. The formation of gold nanoparticles was visually observed through a change in the colour of the solution confirmed by a broad absorbance peak centered at 520 nm in the UV-vis spectrum. Upon interaction with synthetic gibberellic acid(GA), there was a bathochromic shift in the Surface Plasmon peak of AuNPs to higher wavelengths. A change accompanied this shift in the colour of the reaction media from wine-red to purple. To determine the efficacy of the developed probe, pure cultures of *R. Solanacearum* were isolated from soils sampled from bacterial wilt infected farms in Kajiado, Kirinyaga, Kiambu and Bomet counties of Kenya, using Casamino acid Peptone-Glucose (CPG) medium with tetrazolium chloride (TZC) at 28°C for 48h. Gibberellins were extracted from the *R. Solanacearum* cultures and characterized using High-Performance Liquid Chromatography (HPLC) and Fourier transform infrared spectroscopy (FT-IR). Significantly ($p \leq 0.05$) varying concentrations of GA_3 were obtained from 10^8, 10^6, and 10^4 CFU/ml of *R. solanacearum* inoculum. The colorimetric probe elicited colour changes from wine-red to purple upon binding selectively with GA-mediated *R. solanacearum*. The results illustrated the use of Surface Plasmon Resonance (SPR) wavelength-shift sensing and visual colour change of wine-red

nanoparticles to purple nanoparticles to detect gibberellic acid mediated *R. solanacearum*. The distinguishable colour change facilitated the development of a simple sensor for bacterial wilt detection. The high sensitivity of gold nanoparticles played a crucial role in designing the simple colorimetric pathogen probe. This study reports for the first time the use of a colorimetric Nano sensor for bacterial wilt pathogen detection in Kenya. These findings are important for earlyand pre-detection of the pathogen by small scale farmers all over the country and contribute to management strategies for bacterial wilt.

CHAPTER ONE

INTRODUCTION

1.1 Horticultural productivity and constraints

Agriculture plays a crucial role in Kenya's rural economy, accounting for 29.3 percent of the country's gross domestic product (GDP) (HCD, 2019). The horticultural sub-sector of agriculture is fast-growing and one of the country's top foreign exchange earners (Anastacia *et al.*, 2011).The domestic value of horticultural production in 2018 amounted to Ksh. 248.47 Billion compared to Ksh. 207.52 Billion in 2017, equivalent to an increase of 19.7 percent. Over the same period, the cultivated area increased by 3.6 percent from 402,796 ha to 417,367 ha, while total production increased by 7.7 percent from 6.217 million tons to 6.696 million tons in 2018 compared to 5.88 million tons in 2017(HCD, 2019). Horticultural crops in Kenya include flowers, fruits and vegetables. Most players are small-scale farmers, implying that the sector is vital in wealth and jobs creation in rural areas (Ongeri, 2014). Soil-borne diseases contribute between 10-20% yield losses annually in the production of economically significant crops such as tomatoes (Yuliar *et al.*, 2015).

1.1.1 Tomato production: importance, production levels and constraints

Tomato (*Lycopersicon esculentum*) is an edible berry belonging to the *Solanaceae* family. It is considered the second most important vegetable crop after potato globally (Food, 2018). It is grown on more than 4.76 million ha with nearly 165 million tons produced worldwide. Asia and Africa account for about 80% of the global tomato area, with about 72% of world output (Ramasamy & Ravishankar, 2018). Kenya is ranked 6th among Africa's leading tomato producers, with a total production of approximately 397007 tons accounting for 14% of total vegetable production and 6.72% of total horticultural crops in the country (Karuku *et al.*, 2017).

1.1.2 *Ralstonia solanacearum:* economic importance and pathogenesis

Ralstonia solanacearum is a soil-borne bacterium causing bacterial wilt disease in economically important crops resulting in severe yield losses (Abdul *et al.*, 2017). The pathogen affects over 400 plant species (Peeters *et al.*, 2013), particularly in the Solanaceae family, including tomatoes, potatoes, capsicums and eggplants. *R. solanacearum* successfully infects its host cropsas soil, water, and or seed pathogen (Wang *et al.*, 2016.) The pathogen locates the host and gains entry through natural openings or wounds, colonizes the cortex, invades the xylem vessels, and reaches the plant's stem and aerial parts through the vascular system (Mansfield *et al.*, 2012).The bacterium multiplies rapidly within the host plant to very high cell densities clogging the waterway leading to wilting and eventually plant death (Aloyce *et al.*, 2017). To manage the effects of bacteria wilt, there is a need to detect the causal organism at the early phases of infection either by developing new methods or improving the existing ones.

1.1.3 Phytohormones as important biomolecules for pathogen detection

In recent years, secondary metabolites, especially synthesized by bacteria, have become very important in biotechnology. These secondary metabolites include plant growth hormones that areproduced in minute amounts. Phytohormones are not only synthesized by higher plants (Shoukry *et al.*, 2018), they have also been produced by fungi (Yürekli *et al.*,1999) and bacteria (Khalid *et al.*, 2004; Martínez-Morales *et al.*, 2003; Martinez-Toledo *et al.*,1988). These studies indicate the existence of microorganisms associated with plant roots in which the production of plant growth-regulating substances has been shown. Rhizospheric bacteria have been found to produce hormones such as auxins, gibberellins (GA), cytokinins, ethylene and abscisic acidunder *in-vitro* conditions (Patel *et al.*, 2015). Gibberellins and gibberellin-like substances are a class of physiologically important hormones (Sciences *et al*., 2013) produced by bacteria as secondary metabolites (Bertolini & Olmos, 2004; Primo *et al.*, 2015). A clear understanding of the interaction process between the host and the pathogen is important in devising tools for detection.

1.1.4. *Ralstonia solanacearum* identification and detection methods

Various methods are employed in *Ralstonia solanacearum* detection and identification, including Enzyme-linked Immunosorbent Assay (ELISA), immunostrip assays, Polymerase Chain Reaction (PCR), and culture in selective media (Paret *et al.*, 2010). These conventional methods employ many techniques (Stevens & Jaykus, 2014) involving extensive sample preparation and analysis. The existing methods for identifying and detecting *Ralstonia solanacearum* present a wide range of limitations in their use (Hennessy *et al.*, 1996). These methods are expensive, time-consuming, and require skilled labour to utilize. Hence the need to develop other strategies that are more rapid, efficient and user friendly.

Gold nanoparticles can bind with a wide range of organic and inorganic molecules (Khan, 2014).Therefore, they help develop tools to detect specific target molecules produced by disease- causing pathogens or pathogens themselves. Gold nanoparticles have successfully been used to develop colorimetric probes to detect bacteria (Verma *et al.*, 2015). For example, DNA-Gold nanoparticle bound probes were developed to rapidly detect DNA genes extracted from *Pseudomonas syringae* pathovars. To this end, specific primers were designed to amplify a sequence located at a region of bacterial genomes called pathogenicity islands. Subsequently, Gold NP probes were added to the PCR-amplified fragment containing the *hrcV* gene. This gave rise to forming a polymeric network of DNA–Gold NPs with a concomitant red-to-purple colour change (Vaseghi *et al.*, 2013).

AuNPs possess excellent optical and electrochemical properties that can be modified to identify pathogens. This emerging nano-based technology can be used as a strategy to exploit the surface properties of gold nanoparticles in developing a method to detect *R. solanacearum*. The use of colorimetric probes has been reported to significantly reduce the time between sample collection and obtaining results (Lazcka *et al.*, 2007). This method is low-cost, simple, and could allow real-time detection. Upon binding selectively with gibberellic acid, a colorimetric probe will elicit colour changes

observable by the "naked eyes" (Ding *et al.,* 2015; Guo, 2012). The peak absorbance wavelength is sensitive to the distance between the nanoparticles. Each particle's surface plasmon resonance becomes coupled and shifts the absorbance spectrum (Willets & Duyne, 2007). The shift can be significant enough to induce a visual colour change. The linear relationship between the concentration of the analyte and the absorbance also gives steady quantitative results. Therefore, colorimetric probes can be tailored to help farmers make knowledge-based and cost-effective decisions on where to plant their tomato crops, allowing pre-and early rapid detection of bacterial wilt in infested soils. This could result in enhanced productivity for most small-holder tomato farmers in Kenya.

1.2 Statement of the Problem

Ralstonia solanacearum causing bacterial wilt is a devastating soil-borne pathogen that limits theproduction of tomato and other Solanaceae crops (Smith, 2015). Bacterial wilt is a significant threat to most horticultural crops that are host to the pathogen and is by far a threat to food security in tropics and subtropics, especially in the rural areas (Tallury *et al.*, 2010) due to limited access to proper agricultural technologies and information. While many methods of detection are available, they possess numerous limitations. Colorimetric probes are suitable for use by rural populations when fully developed due to their simplicity, low cost, rapidresults, and do not require apparatus. Conventional pathogen detection methods include microbiological and molecular methods (Champoiseau *et al.*, 2009). Colony counting involves the isolation and growth of the suspect pathogen. Initial results require at least two days with confirmation after 7-10 days (Verma *et al.,* 2015). Immunological assays depend on antigen recognition of antibodies involving multiple steps, specialized training, and several hours of run time (Lazcka *et al.,* 2007).

On the other hand, PCR-based methods rely on various detection schemes that depend on nucleic acid amplification to increase the detection target's concentration. The main disadvantage of traditional PCR-based methods is the inability to distinguish viable and non-viable cells since both contain the amplification target molecule (Velusamy *et al.*, 2012). These methods give slowdata output, require complex sample handling, and use

high-cost instruments. Errors also arise during handling because they require extensive sample collection, transportation, and pretreatment (Stevens & Jaykus, 2014). A more practical and integrated approach for preventing systemic diseases is early detection to reduce yield losses during production. This, therefore,calls for the development of methods that are simple, selective, and easy to use by non-skilled farmers in the field.

1.3 Justification

Crop losses can be reduced, and specific treatments developed to control the disease pathogen if the disease is accurately diagnosed and identified before spreading. Biosensors can overcome limitations presented by conventional methods by miniaturizing devices and providing simple results without the need for specialized training/skilled personnel (Lazcka *et al.*, 2007). Nano-based colorimetric probes can overcome some of the various limitations arising from the use of conventional detection methods (Hadi *et al.*, 2018). Colorimetric probes can be defined as materials that bind selectively with the analyte to give a distinctive colour change. They are attractive in research and have received considerable attention in the recent past due to their simplicity, low cost, rapidity, and hence very attractive (Bertolini & Olmos, 2004). Nanomaterials, organic dyes and synthetic ligands are used to successfully fabricate colorimetric probes (Lin *et al.*, 2011). Metal nanoparticle-based colorimetric assays do not utilize organic co-solvents, enzymatic reactions, light-sensitive dye molecules, lengthy protocols or sophisticated instrumentation, therefore, overcoming some of the limitations posed by conventional methods. Gold nanoparticles are suitable materials for assembling colorimetric probes due to their colour, mainly based on the surface plasmon resonance and the display of distant dependent optical properties (Jongjinakool *et al.*, 2014). Dispersion or agglomeration of AuNPs due to the presenceof targeted analyte results in a distinctive colour change which is a sensing mechanism for detecting various biomolecules (Park *et al.*, 2014). Dispersed AuNPs are red, whileagglomerated ones are purple or blue. Colorimetric probes using metal nanoparticles, for instance, have been explored and bear critical applications in the successful and sensitive detection of metal ions in various matrices using the above mechanism (Priyadarshini & Pradhan, 2017).

Therefore, this study aimed to develop a user-friendly colorimetric probe using gold nanoparticles to detect Gibberellic acid exuded by bacterial wilt of tomato causative agent, *R. solanacearum*. The study exploited the large reactive and the exposed surface of gold nanoparticles in designing a probe with sensing properties for field use by unskilled and skilled farmers.

1.4 General objective

To develop and validate a probe for detection of *Ralstonia solanacearum* causing bacterial wilt in tomato for enhanced disease management in Kenya

1.4.1 Specific objectives

i. To develop a probe based on gold nanoparticles for detecting *Ralstonia solanacearum*

ii. To determine the sensing mechanism of the colorimetric probe in detecting Gibberellin-mediated *Ralstonia solanacearum*

iii. To validate the developed colorimetric probe in detecting *Ralstonia solanacearum* isolates from selected Bacterial wilt endemic counties.

1.5 Null Hypotheses

$H_0$1: The gold nanoparticle-based colorimetric probe cannot detect *Ralstonia solanacearum.*

$H_0$2: The colorimetric probe sensing mechanism is not dependent on Gibberellin-mediated *Ralstonia solanacearum* exudation

$H_0$3: The developed colorimetric probe cannot detect *Ralstonia solanacearum* from Bacterial wilt infested soils

CHAPTER TWO

LITERATURE REVIEW

2.1 Overview/Introduction

This chapter presents background information on tomato production in Kenya and its economic importance, Epidemiology and bacterial wilt disease symptomatology, existing methods available for detecting bacterial wilt, Mechanisms and, the theory of colorimetric probes and metal nanoparticles.

2.2 Tomato production

Tomato (*Solanum lycopersicum* L.) is an important food and industrial crop, cultivated all over the world. The species originated in western South America and Central America and numerous varieties of the tomato plant are widely grown in temperate climates across the world, with greenhouses allowing for their production during all seasons of the year. Tomatoes are fruits, botanically classified as berries. They are commonly used culinarily as a vegetable ingredient. It is an essential component of human diets (Anang *et al.,* 2013), providing a rich source of vitamins and minerals, particularly lycopene (60–90 mg/kg). The horticulture sub-sector of agriculture has become a vital income source for small-holder farmers, government revenue, and foreign exchange earnings in Kenya (Mwangi *et al.,* 2020). Tomato is the leading exotic vegetable produced in Kenya and a promising commodity in horticultural expansion (Karuku *et al.,* 2017). Small-holder farmers with farms ranging between 0.2 to 3ha account for approximately 70% of total agricultural output (Ndirangu *et al.,* 2018). Tomatoes are grown in areas with altitudes that range from 1150 and 1800m above sea level. Tomato was the leading vegetable produced in 2018, accounting for 37.63% of all the exotic vegetables produced in Kenya. The revenue earned from tomatoes increased from Ksh.17.38billion in 2017 to Ksh.19.90 billion in 2018, representing a 14.5 percent increase. The acreage grew from 27,053ha in 2017 to 28,263 in 2018, a 4.5percent increase, while production increased from 507,275tons to

574,458tons, a 13.2 percent increase. The growth in the area under tomato production, volume and revenue in 2018 was attributed to enhanced irrigation and growing of hybrid varieties that are high yielding and tolerant to pests and diseases (HCD, 2019) (Table 2.1).

Table 2.1: Production of Tomato in Kenyan counties from 2017- 2018

COUNTY	2017			2018			% Of
	Area (Ha)	Volume (MT)	Value (KES)	Area (Ha)	Volume (MT)	Value (KES)	Total
Kajiado	2,452	54,827	1,914,835,250	3,024	71,250	2,379,680,250	12.0
Kirinyaga	3,219	60,490	2,247,500,000	2,460	60,587	2,037,800,000	10.2
Narok	2,277	54,220	1,700,200,000	2,420	54,082	1,886,227,500	9.5
Machakos	2,453	39,255	1,029,775,000	4,075	56,225	1,328,475,000	6.7
Kiambu	544	7,099	270,033,750	769	24,499	1,249,126,000	6.3
Taita Taveta	726	22,990	904,500,000	783	28,610	1,238,650,000	6.2
Makueni	575	22,250	893,600,000	931	27,675	941,600,000	4.7
Homabay	1,143	8,490	482,811,240	1,541	12,104	743,706,000	3.7
Lamu	275	10,700	242,508,000	491	16,242	693,153,000	3.5
Kisumu	663	16,341	542,320,000	536	19,030	592,650,000	3
Trans Nzoia	672	19,804	613,560,000	441	14,633	518,266,000	2.6
Kitui	311	6,743	245,790,000	735	13,588	459,685,000	2.3
Murang'a	1,258	8,888	417,409,550	1,315	9,250	448,946,300	2.3
Bungoma	538	10,041	456,710,000	564	11,129	442,570,000	2.2
Siaya	741	10,674	442,675,000	628	9,523	431,532,500	2.2
Laikipia	578	19,670	674,420,300	321	10,999	376,500,000	1.9
Bomet	545	7,535	236,650,000	550	9,849	320,578,000	1.6
Kwale	448	6,989	320,023,000	420	6,966	319,660,000	1.6
Meru	549	12,386	485,356,018	498	9,702	316,985,000	1.6
Nyeri	273	6,670	239,619,940	356	11,348	299,950,768	1.5
Others	6,812	101,214	3,018,982,134	5,405	97,167	2,877,810,938	14.5
Total	**27,053**	**507,275**	**17,379,279,182**	**28,263**	**574,458**	**19,903,552,256**	**100**

Source: AFA-Horticultural Crops Directorate, 2019

2.3 Bacterial wilt disease

Bacterial wilt of Tomato is one of the most severe soil-borne pathogens in Kenya that limits Tomato and other Solanaceae crop production (Ireri *et al.,* 2018), resulting in substantial yield losses threatening food and economic security. The disease is caused by *Ralstonia solanacearum,* a destructive bacterial pathogen of plants (Mansfield *et al.*, 2012) with a broad host range of economically important plants such as tomato, potato, eggplant and many other crops within the solanacearum family (Monteiro *et al.*, 2012). The *β*-proteobacterium (formerly *Pseudomonas solanacearum*) is a species complex whose strains are classified as phylotypes andbiovars according to their molecular and biochemical profile, respectively (Álvarez *et al.*, 2008). The pathogen is challenging to control due to its ability to grow endophytically and survive in conducive soil conditions, especially in the deeper layers, travel along the water, and its relationship with weeds

2.3.1 Geographical distribution and host range

Bacterial wilt has a worldwide distribution, affecting crop production in tropical, subtropical, andtemperate regions (Champoiseau, 2008). In Africa,it is found in Angola, Burkina Faso, Burundi, Cameroon, Congo, Ethiopia, Gabon, Gambia, Kenya, Madagascar, Malawi, Mauritius, Mozambique, Nigeria, Rwanda, Senegal, Seychelles, Sierra Leone, Somalia, South Africa, Swaziland, Tanzania, Tunisia, Uganda, Zaire, Zambia, and Zimbabwe ("EPPO," 2004). It displays a broad host range of more than 450 species in 54 botanical families, including monocots and dicots (Aloyce *et al.*, 2017; Fegan *et al.*, 2005; Muthoni *et al.*, 2012). Direct yield losses by *R. solanacearum* vary widely according to the host, cultivar, climate, soil type, cropping pattern, and strain, e.g., 10 to 91% in Tomato and 10 to 30% intobacco (Yuliar *et al.*, 2015). The disease's economic impact occurs in infected tomato, potato, banana, ginger, groundnut, and capsicum crop fields. The bacterium has also raised serious concerns in the floriculture industry, especially geranium production. Further, *R. solanacearum* pathogen has a quarantine status in the European Union (E.U.) due to its lethality, broad host range, and wide geographical distribution.

2.3.2 *Ralstonia solanacearum* pathogenesis

The infection begins with attachment to host roots, followed by microcolonies on the root surface. In the environment, *R.solanacearum* senses specific stimuli (mainly root exudates), moves towards the host roots by swimming motility and attaches to the host root. *R. solanacearum* evades root defences such as nucleic acid extracellular traps and gains entry into hosts through wounds (e.g., Root-Knot nematodes) or natural openings on roots moving through the cortex into the xylem vessels. The pathogen rapidly colonizes its preferred niche, the water- transporting xylem vessels, and multiplies extensively, producing large amounts of exopolysaccharide (EPS) (Lowe-Power *et al.,* 2016). EPS consists of a complex polymer of N-acetylated sugars. EPS contributes to virulence by blocking xylem vessels and was recently found to trigger defence responses in bacterial wilt- resistant tomato plants specifically (Milling *et al.,* 2011). It is hypothesized that *R. solanacearum* requires EPS to form biofilms on vessel surfaces during disease development to survive desiccation/antibiosis in the soil during the absence of host plants. EPS protects *R. solanacearum*from plant antimicrobial defences by cloaking bacterial surface features that hosts could recognize (Denny, 2015). In the xylem, *R. solanacearum* grows to high cell densities (10^9 CFU/g stem), reducing the xylem sap flow, causing wilting and eventually host death. While inside the host, *R. solanacearum* deploys virulence factors such as plant cell wall degrading enzymes, type 3 secreted effectors, and extracellular polysaccharides. The primary virulence determinant is the type III secretion system (T3SS) (Gijsegem *et al.,* 1993), which injects several effector proteins into plant cells, causing host disease or a hypersensitive responsein resistant plants.

Once the host plant dies, the bacterium is released to a saprophytic life in the soil or other environment. It survives using diverse strategies such as; Viable but Non-culturable forms (VBNC state), starved cells, PC-type, and biofilms until a new host appears (Champoiseau, 2008).

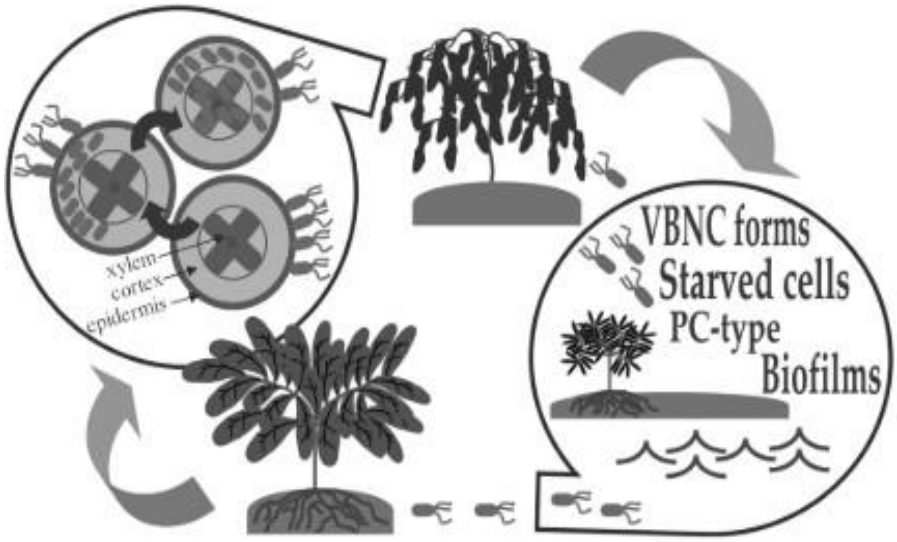

Figure 2.1: The life cycle of Ralstonia solanacearum inside and outside the host. Source:*(Champoiseau, 2008)*.

2.3.3 Epidemiology and symptomatology

The age of the plant and point of inoculation influence the incubation period in the field from infection to when typical symptoms are expressed, ranging from days to several weeks. The bacterial wilt spread in an area is most rapid while plants are young and succulent and decreaseas the plants mature. Weather and ideal growing conditions such as warm weather, adequate soil moisture, sunlight, and balanced nutrient concentrations may also favour the disease's development (Dalsing & Allena, 2014). The pathogen colonizes the root cortex and vascular parenchyma's intercellular space, enters the xylem vessels, and then spreads up into the stem andleaves (Flores-Cruz & Allen, 2011). Xylem becomes fully colonized, and masses of bacterial cells are shed from the roots providing a pathway for bacteria to return to the soil and initiatenew infections. Symptoms of bacterial wilt in tomato plants include yellowing, stunting, and wilting (N'Guessan *et al.*, 2012). The youngest leaves of the tomato plant are the first to be affected. They show a flaccid appearance, usually at the hottest time of day. When environmental conditions are conducive to disease progression, the entire plant's wilting may follow rapidly. Under less favourable conditions, the disease develops less rapidly, stunting may occur, and

many adventitious roots attributed to interference with downward movement in phloem resulting from effects of pathogen (Buddenhagen *et al.*, 1982). Slimy viscous ooze appears on cut transverse-sectioned stems at the points corresponding tos the vascular bundles. Eventually, the host plant collapses and dies because it cannot take up water (Álvarez *et al.*, 2010; "Ralstonia solanacearum," 2004).

2.4 Conventional methods for detection of Bacterial wilt and significant challenges in theiruse

Detection establishes a particular target organism within a sample, emphasizing symptomless individuals. Existing methods used in *R. solanacearum* detection and identification include Serological assays, e.g., Enzyme-linked immunosorbent assay (ELISA), serological detection techniques, culturing and physical observation (Bertolini & Olmos, 2004; Gatahi *et al.*, 2017; Yuliar *et al.*, 2015). These methods often offer good sensitivity and specificity. The major disadvantages are the required processing times, high-cost equipment, and the need for skilled labour. Most of the time, complex hyphenated techniques have to be employed (Davis *et al.*, 2015). Physical observation of bacterial wilt is only possible after severe crop infestation resulting in considerable losses. *R.solanacearum* can be identified from either symptomatic or asymptomatic plants. Screening tests such as bacterial streaming, plating on selective medium, nucleic-acid-based identification using *R.solanacearum* specific primers, and pathogenicity assessment using susceptible hosts (e.g., tomato seedlings) can also be used for early detection and identification of bacteria in infected plants or contaminated soil and water samples.

2.4.1 Molecular detection methods

Molecular techniques based on hybridization or amplification are available for significant plant pathogenic viruses and bacteria (Bertolini & Olmos, 2004).

2.4.1.1 Fluorescence in situ hybridization

Fluorescence in situ hybridization (FISH) is used for bacterial detection by combining microscopy observation and hybridization specificity (Kempf *et al.*, 2000). Its detection of plant pathogenic bacteria depends on DNA probes' hybridization to species-specific bacterial ribosome regions. They are particularly attractive as diagnostic targets because ribosomal RNA has functional sequences common to all species and specific to individual species. FISH only needs to recognize this particular information.

2.4.1.2 Polymerase Chain Reaction

Polymerase Chain Reaction (PCR) is a nucleic acid amplification technology widely used in bacterial detection. It is based on nucleic acid amplification to increase the concentration of the detection target of the isolation. Examples of different PCR methods developed for bacterial detection are (i) real-time PCR, (ii) multiplex PCR, and (iii) reverse transcriptase PCR (RT- PCR). The target deoxyribonucleic acid (DNA) sequences are amplified, enabling a high sensitivity and detecting single gene copies. The sensitivity can be easily achieved without a prolonged incubation because there is no need to grow the bacteria (Ahmed *et al.*, 2014).Specificity is achieved because the primers are designed for target sequences unique to the pathogen of interest. However, interference may occur from non-pathogenic genetic material, resulting in a mismatch or non-specific amplification. Precise genetic information is therefore required for confidence in the results obtained using this technique. After amplification, samples are traditionally separated by gel electrophoresis. Extensive sample preparations increase labour costs and processing times (Lazcka *et al.*, 2007). It takes 5 to 24 h to produce a detection result, but this depends on the specific PCR variation used, which does not include any previous enrichment steps. The main drawback of traditional PCR-based pathogen detection methods is their inability to distinguish between viable and non-viable cells since both containthe amplification target. Detection of bacteria or viruses in a given sample by PCR depends on the performance of the PCR assay and the efficiency of the procedure employed to extract the plant material's nucleic acids.

2.4.2 Culture and colony counting methods

The culturing and plating method is the oldest bacterial detection technique and remains the standard pathogen detection method. It usually involves isolation and growth of a suspectpathogen on selective media, followed by visual observation of colonies under a microscope and confirmation based on existing literature. Different selective media are used to detect particular bacteria species. They can contain inhibitors (to stop or delay the growth of non-targeted strains) or distinct substrates that only the targeted bacteria can degrade or confer a particular colour to the growing colonies (Fratamico, 2003). Plating assays provide information about the number of viable cells, expressed as colony-forming units, but are time-consuming and laborious (Chitarra & Van Den Bulk, 2003). This method is only advantageous for identifying organisms that occur at low levels (i.e., single cells). This process, however, is time-consuming because of long incubation periods and requires skilled labour. Four to nine days are needed to obtain a negative result, and between forteen and sixteen days to confirm a positive result (Brooks *et al.*, 2004). A pathogen also must be culturable for this technique to be applicable in its identification.

2.4.3 Serological detection methods

2.4.3.1 Monoclonal and recombinant antibodies

The specificity of detecting bacteria by serological techniques such as ELISA has significantly improved with specific monoclonal and recombinant antibodies, which allows the selection of particular target epitopes, hence avoiding false positives. However, specificity problems arise during analysis when bacteria are present in the plant material, soil, and water, and large quantities of other microorganisms are also present in the sample. Commercial monoclonal antibodies, which have available specific monoclonal antibodies, are available such as Agdia (Elkhart, Ind.), Adgen (Ayr, UK), and Agritest (Valenzano, Italy). These methods providesignificant time and cost advantages (Terrada *et al.*, 2000). However, their applications for diagnostic purposes are still scarce.

2.4.3.2 Enrichment-ELISA protocols

Combining ELISA, which uses specific monoclonal antibodies, improves the sensitivity ofdetecting bacterial pathogens with a preliminary enrichment step (Llop & Cubero, 2001). This methodology has been developed because of ELISA's low sensitivity for bacterial detectionusing specific monoclonal antibodies (maximally 10^5–10^6 CFU/ml) and the need to improve this sensitivity, especially to detect latent infections of quarantine bacteria.

2.4.3.3 On-site-testing: tissue print-ELISA and lateral flow devices

Commercial methods for rapid detection are needed for testing many samples by unskilled personnel. As a result, a number of tissue print- ELISA and lateral flow devices have been developed for economically important plant viruses and bacteria. When using suitable monoclonal antibodies, specificity is very high, especially during virus detection. However, it is relatively low for bacteria, thus limiting its application. They are more suitable for analyzing plants with symptoms.

2.4.3.4 Flow cytometry

This technique identifies cells or other particles passing individually through a specific sensor, usually in a liquid stream. Using fluorescent dyes conjugated to specific antibodies, bacterial cells are identified rapidly. The bacterial cells are detected electronically using a fluorescence- activated cell sorter that measures cellular parameters based on light scattering and fluorescence. The multiparameter analysis includes cell sizing, fluorescence imaging, gating out, or eliminating unwanted background associated with dead cells and debris. The cost of instrumentation involved in this technique is a significant drawback (Chitarra & Van Den Bulk, 2003).

2.4.4 Physical observation of bacterial wilt symptoms

Conventional field scouting of plant diseases and pests is labour-intensive, prone to be subjective, and generally low efficiency (Zhang *et al.*, 2019). The traditional method of identifying plant pathogens through physical observation is only possible after crop damage, thus limiting the effectiveness of any remedial strategy.

2.4.5 Diagnostic probes for the determination of bacteria

Rapid, accurate, and early detection of pathogenic bacteria is essential for early diagnosis and prevention. Both colorimetric and fluorescent molecular probes possessing appropriate functionalities have consistently demonstrated their potential to analyze cations, anions, and neutral species, both qualitatively and quantitatively.

2.4.5.1 Fluorescent probes

Fluorescence is the emission of radiation from specific molecules, called fluorophores, after appropriate excitation. A fluorescent probe, also called fluorescent dye, is a fluorophore designedto localize a particular biological specimen region or respond to a specific stimulus (Poot *et al.*, 1996). A colorimetric probe will elicit colour changes that the "naked eyes" can observe upon adding the target microorganism. Similarly, fluorescent changes produced by fluorescent probes can be detected using a fluorometer or even more conveniently under a portable UV lamp, showing higher sensitivity. The fluorescence technique has advantages over other instrumental methods because it does not require extensive sample preparation; hence, it is relatively fast. A common strategy for developing such a probe is linking a recognition unit to a signal reporting chromophore, such as anthracene, fluorescein, courin rhodamine, boron dipyrromethene (BODIPY), porphyrin, and cyanine dyes. A large number of fluorescent probes are available to study the properties of microorganisms (Chitarra & Van Den Bulk, 2003).

2.4.5.2 Colorimetric probes

Colorimetric probes, as previously described, are materials (biotic/abiotic origin) that bind selectively with the desired analyte in a reaction to give a distinctive colour change(Cu *et al.*,2007). Colorimetry is a solution-based assay method that can estimate the concentration ofthe material in the solution by measuring the absorption wavelength (Jazayeri*et al.*, 2018). Colorimetric probes are considered attractive as sensing devices because they involve simple visual detection techniques, allow a rapid and sensitive determination to the "naked eyes" on- site, and does not require sample pretreatment (Godoy-reyes & Costero, 2019). The apparent colour change of the sample makes the testing direct and convenient. The linear relationship between the bacteria molecule concentration and the absorbance also shows steady, quantitative results (Raj *et al.*, 2015). Colorimetric probes can overcome the limitations presented by traditional instrumental methods because no sophisticated instrumentation or sample preparation is required in their procedures. The successful use of colorimetric probes is attributed to the low cost involved to develop and simple-to-use diagnostic tool for detecting a wide range of molecules.

In colorimetric probes, incorporating an optical signaling moiety close to a host binding site allows the host to act as a prototype for a target guest species. Binding perturbs its electrochemical and photophysical properties hence a bathochromic or hypsochromic shift of absorption spectra. A visual colour change is also effected by the respective increase or decrease in electron densities on the chromophore moiety (Scheme 2). Colorimetric sensors bring about a change in colour and SPR absorbance peak, either due to analyte induced particle aggregation or disassembly of aggregated particles (Priyadarshini & Pradhan, 2017). Many materials havebeen used in the fabrication of colorimetric probes, and these include; organic dyes, synthetic ligands, nanomaterials (i.e., TiO_2 NPs, SiO_2 nanoparticles, quantum dots (e.g., CdSe and CdTe); AuNPs, AgNPs, CuNPs (Lin *et al.*, 2011a). Colorimetric probes using noble metal nanoparticles, usually Silver (Ag) or Gold (Au), have received considerable attention in the recent past due to

their; simplicity, low cost and rapidity. They are well known for their strong interactions with visible light through the resonant excitations of the conduction electrons' collective oscillations within the particles (Su *et al.*, 2003).

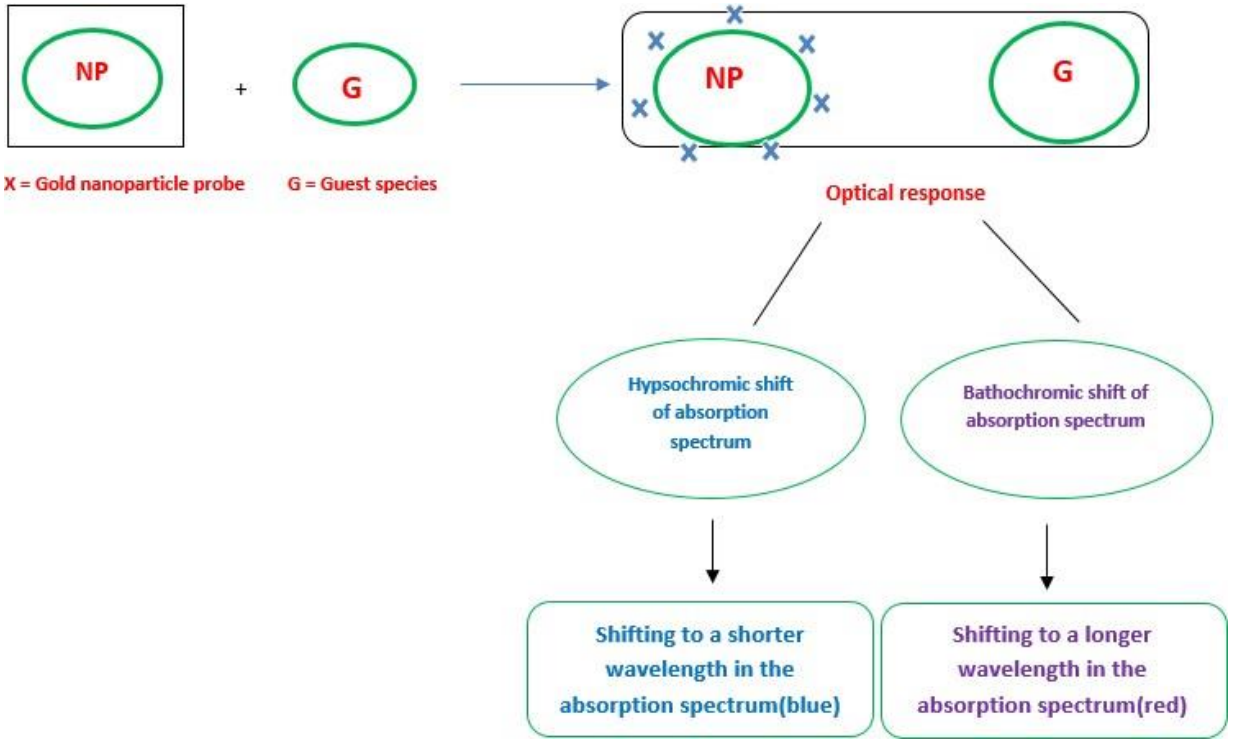

Figure 2.2: Schematic presentation of hypsochromic and bathochromic shifts of a compound's absorption spectrum (Source: (Verma, Singh, & Chavan, 2014a)

2.4.6 Nanoparticles

Nanoparticles are particles with sizes ranging from 1 to 100 nm. They possess a high surfacearea per unit volume, a high proportion of atoms in the surface and near-surface layers, and the ability to exhibit quantum effects. Nanoparticles have great chemical diversity in metals, metal oxides, semiconductors, polymers, carbon materials, organics or biological. They also exhibit great morphological diversity with shapes such as

spheres, cylinders, disks, platelets, hollow spheres and tubes, etc. (Vilela *et al.,* 2012). Nanoparticles are generated via several synthetic routes based on gas, liquid or solid-phase approaches. The synthesized nanoparticles have to be surface modified in most cases to stabilize them since their nanoscale dimensions render them chemically very reactive and physically aggregative. The nanoparticles are also surface- functionalized to meet the needs of specific applications (Andres *et al.,* 2008). Nanoparticles serve as the fundamental building blocks for various nanotechnology applications. The combination of nanotechnology with chemistry, biology, physics, and medicine for the development of ultrasensitive detection and imaging methods in the analytical or biological sciences is becoming increasingly important in modern science (de la Rica *et al.*,2012; Niemeyer, 2002; Rosi & Mirkin, 2005; Stewart *et al.,* 2008).

2.4.6.1 History of metal nanoparticles

Metal nanoparticles have been in use for a long time, such as the Lycurgus Cup manufactured in the 5^{th} to 4^{th} century B.C. It is ruby red in transmitted light and green in reflected light to the presence of gold colloids. The extraction of gold started in the 5^{th} millennium B.C near Varna (Bulgaria) and reached 10tons per year in Egypt around 1200-1300BC when the marvellous statue of Touthankamon was constructed (Andres *et al.,* 2008).

Figure 2.3: Nanoparticles in ancient materials: a) Lycurgus Cup in the British Museum (Red colour from nano-sized gold), b) Pottery Of Deruta (Umbria, Italy) (Glazes containing copper and silver nanoparticles.

2.4.6.2Metal nanoparticles

Noble metal nanoparticles are employed in many applications due to their unique optical and physical properties and their interactions with incident light (Teow & Mohammad, 2019). They are attractive because of their size and shape-dependent properties. Metal nanoparticles, particularly silver and gold nanoparticles with well-controlled size, have recently been the focus of great interest because of their colour changes. The colour changes are associated with their surface plasmon absorption band, which depends on many parameters, e.g., the shape and size of the particle, the adsorbed species, the dielectric properties of the medium, and the distance between particles (Tsegay *et al.*, 2019). For a successful colour signal generation, metallic NPs possess much higher extinction coefficients than organic dyes, making them attractive. This allows sensitive colorimetric detection of various molecules with minimal material consumption

(Khodashenas *et al.,* 2021). More importantly, the distance-dependent optical properties of NPs can be easily exploited in scolorimetry (Chen *et al.,* 2012), e.g. dispersed gold nanoparticles are red, while aggregated ones are purple or blue.

2.4.6.3 Silver and copper nanoparticles

Of the three metals (Ag, Au, and Cu) that display plasmon resonances in the visible spectrum, Ag exhibits the highest efficiency of plasmon excitation. Moreover, optical excitation of plasmon resonances in nano-sized Ag particles is the most efficient mechanism by which light interacts with matter. Silver nanoparticles interact with light more efficiently than a single particle of the same dimension composed of any known organic or inorganic chromophore. The light- interaction cross-section for Ag can be about ten times that of the geometric cross-section, whichindicates that the particles capture much more light than is physically incident on them. Silver is also the only material whose plasmon resonance can be tuned to any wavelength in the visible spectrum (Evanoff & Chumanov, 2005).

On the other hand, copper costs significantly less than silver and gold; therefore, it is economically attractive. Due to their unique physical and chemical properties and low-cost preparation, copper nanoparticles have been of great interest recently. The key to metal nanoparticles colorimetric sensing platform is controlling their dispersion and aggregation behaviour. Several stabilizing and capping agents have been used to direct the growth of nanoparticles during synthesis to control the inter-particle distance.

2.4.6.4 Gold nanoparticles

Gold nanoparticles possess several properties, such as facile reactivity with biomolecules, high surface area to volume ratios, and distance-dependent optical properties. Such properties make them ideal for colorimetric probe development (Andres *et al.,* 2008). AuNPs are also highly inertand stable against oxidation and can be synthesized using numerous physicochemical and biological routes (Syed & Bukhari, 2011). The peak

absorbance of gold nanoparticles is greatly influenced by their size and shape and is sensitive to particles' distance. When aggregation occurs, the SPR of the individual particles becomes coupled and shifts the absorbance spectrum (Verma *et al.*, 2014b). This shift produces a visible colour change, making the technique favourable for rapid and on-site detection. Peak absorbance wavelengths exhibit a redshift with increased size, giving red stable (non-aggregated) nanoparticles while aggregated nanoparticles appear blue or purple. An ultraviolet-visible spectrophotometer can help quantify the SPR peak shift (Jazayeri. *et al.*, 2016).

2.4.7 Synthesis of AuNPs

2.4.7.1 Chemical Synthesis of AuNPs

Numerous preparative methods for AuNPs have been reported, including both "top-down" (physical manipulation) and "bottom-up" (chemical transformation) approaches (Alex & Tiwari, 2015; Marie-Christine & Didier, 2004). The top-down approach involves synthesizing AuNPs starting from bulk material and cracking it into nanoparticles using different methods. In contrast, the bottom-up approach synthesizes nanoparticles starting from the atomic level. These methods include the Turkevich method, the Brust method and seed-mediated growth and they arebriefly described below.

2.4.7.1.1 Turkevich method

It is a commonly used technique for the formulation of spherical AuNPs, and it involves:

(i) Reduction of a gold ion (Au^{3+}), which will be a gold salt solution, with reducing agents like amino acids (Bajaj *et al.*, 2018), ascorbic acid (Niidome *et al.*, 2003), UV light and borohydrides or citrate (Kumar *et al.*, 2007)to produce gold atoms (Au^{0})

(ii) Stabilizing the obtained AuNPs by suitable stabilizing or capping agents like citrate or alkane thiols prevent nanoparticles' aggregation from forming metallic precipitate (Alex & Tiwari, 2015).

By varying the ratio of reducing and stabilizing agents, AuNPs of a particular size range from 16–147 nm could be produced (Clarke&Bailey, 1973). Scheme 2A shows the primary method involved in the Citrate reduction method.

The Turkevich method is a relatively uncomplicated and reproducible procedure for the formulation of spherical particles with a size range of 10–30 nm. With an increase in size above 30 nm, they become less spherical with broader size distribution. Moreover, this reaction gives a low yield and uses only water as a solvent (Dong *et al.*, 2020).

2.4.7.1.2 The Brust Method

This method is a two-step process used to synthesize AuNPs using organic solvents. This method encompasses using a phase transfer such as tetraoctylammonium bromide to transfer gold salt to organic solvent from its aqueous solution (e.g., toluene). The gold is reduced by using a reducing agent such as sodium borohydride and alkanethiol. The alkanethiol carries out the stabilization of AuNPs (Brust *et al.*, 2000). Scheme 2B shows the schematic illustration of the main steps involved in the Brust method.

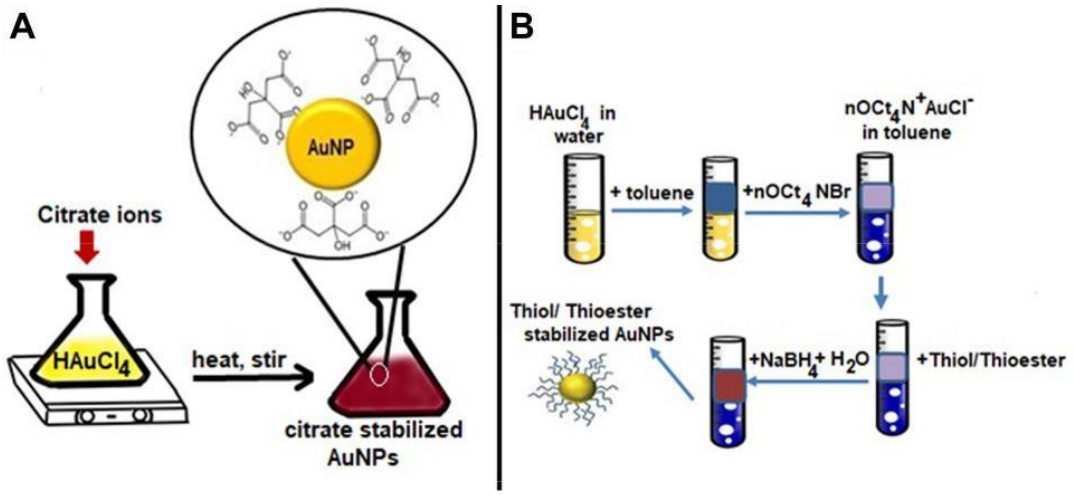

Figure 2.4: (A) Turkevich method for the synthesis of AuNPs. (B) Series of steps involved in theBrust method for the synthesis of AuNPs. Source: Amina & Guo, 2020.

The Brust method involves formulating thermal and air-stable AuNPs having controlled size and less dispersity. One possible limitation of the Brust method is the synthesis of AuNPs that areless dispersed, limiting their biological applications (Herizchi *et al.*, 2016)

2.4.7.1.3 Seed-mediated growth

The Turkevich and Brust methods can synthesize only spherical AuNPs; however, at times, AuNPs can also be formulated in several geometries and shapes, such as rods (Ying Chen *et al.*, 2005). The most commonly used technique to synthesize rod-shaped AuNPs is seed-mediated growth. Seed particles are synthesized using reducing agents like $NaBH_4$. This is followed by transferring the seed particles to a metal salt and a weak reducing agent such as ascorbic acid, which speeds up the synthesis of rod-shaped AuNPs and prevents further agglomeration (Amina & Guo, 2020).

Seed-mediated growth is a reliable method for synthesizing rod-shaped AuNPs, but factors that affect the size of the rod must always be carefully monitored.

2.4.7.2 Biological synthesis of AuNPs

Recently, efforts have been made for the biological synthesis of AuNPs. It is a clean and biologically friendly alternative to the harsh chemicals used in chemical and physical synthesis reactions (Song *et al.*, 2009). Biological methods for nanoparticle synthesis range from plants or plant extracts microorganisms, algae to complex eukaryotes (Amina & Guo, 2020; Song *et al.*, 2009).

2.4.7.2.1 Biosynthesis of AuNPs using plants

Several studies have reported the biosynthesis of AuNPs using different plants or simple plant extracts. The process involves using harmless bio components from plants to carry out the reduction and stabilization of AuNPs. This results in reducing waste and limits the requirement for additional purification steps. The functional groups of flavonoids, phytosterols and quinones present in plants are involved in the synthesis of AuNPs by

speeding up the reduction and stabilizing AuNPs(Lee *et al.,* 2020). For example, a study reported the fruit of *Citrus maxima*, synthesized AuNPs with the size range of 15-35nm with ascorbic acid, proteins, and terpenes assumed to be the reducing agent in the reaction (Yu *et al.,* 2016). In another study, *Mangifera indica* leaves synthesized spherical AuNPs in size range 17-20nm within 2minutes of the reaction time. Terpenoids, flavonoids and, thiamine were the active compounds that might have contributed to the synthesis of AuNPs (Philip, 2010). Synthesis of AuNPs using plant-based material is a simple process. Properties such as shape and size can be controlled by regulating the reaction conditions. Additionally, the reaction process is fast and economical. The major limitation is identifying reactive components, which is complex since plant biomass constitutes many organic components (Bogireddy *et al.,* 2018).

2.4.7.2.2 Biosynthesis of AuNPs using bacteria

The negatively charged cell wall of bacteria can electrostatically interact with positively charged Au(III) ions. Gold ions are transported inside the cell, where enzymes and biomolecules carryout the intracellular synthesis of AuNPs. On the other hand, the gold ions are trapped on the cell membrane by membrane enzymes during extracellular synthesis. (Li *et al.,* 2011). It was reported by Ahmad *et al.,* 2003, that *Thermomonospora sp.* (Order: Actinomycetes) achieve the reduction of Au(III) ions at the surface of membrane and mycelia via intracellular enzymes producing AuNPs. This process is tedious and requires precautionary measures while handling bacteria. It also takes hours and days as bacterial culture is time-consuming. These drawbacks have limited the use of bacteria for the synthesis of AuNPs (Ovais *et al.,* 2018). The extracellular synthesis approach in bacteria produces pure nanoparticles compared to the intracellular synthesis process, which requires additional purification steps. However, culturing bacteria is a slow process, so the synthesis of AuNPs can take an extended period.

2.4.7.1.1 Biosynthesis of AuNPs using fungi

Fungi secrete a number of biomolecules, including metabolites and extracellular enzymes, whichhave been reported to play a role in synthesizing metallic nanoparticles. Studies by Senapati *et al.*, 2005 showed that a fungal species, *Fusarium oxysporum*, was used in the extracellular synthesis of AuAg alloy NPs by the reduction action of nitrate-dependent enzyme and shuttle quinone. Fungi produce many proteins and reactive compounds, allowing the reaction process to be easily scaled up (Ganaie *et al.*, 2014). However, preparing biomass from fungi for thesynthesis reaction requires careful steps as separating mycelia from culture filtrates is complicated.

2.4.7.2.4 Biosynthesis of AuNPs using biomolecules

Macromolecules such as amino acids, nucleic acids, carbohydrates, and lipids are synthesized by living organisms to speed up their biological processes and are referred to as biomolecules. Other similar studies have reported the synthesis of gold nanoparticles using chitosan, which acts as a reducing agent and as a stabilizing agent during synthesis reaction (Esther & Sridevi, 2017). Starch is also a polysaccharide used in the synthesis of AuNPs. In an alkaline environment, starch can be degraded into short chains having carboxyl groups and the –OH group of carboxylic acid can reduce Au^{3+} ions to gold nanoparticles (Pienpinijtham *et al.*, 2012). Biomolecules contain various functional groups which can aid in the synthesis of AuNPs. Biomaterials, however, exhibit varying reducing abilities. First, establish their reducing ability before using them in the AuNP synthesis reaction (Yijun Chen *et al.*, 2017; Geng & Grove,2015; J. Lee *et al.*, 2011; Saha *et al.*, 2017).

2.4.7 Stabilization and functionalization of metal nanoparticles

Nanoparticles (NPs) are thermodynamically unstable because their large surface-to-volumeratios result in high reactivity and the need for stabilization (Gommes, 2019). When nanoparticles are not stabilized, they will generally undergo a process known as

"Ostwald Ripening". Ostwald ripening is a significant source of deactivation of functional nanomaterials. It is the tendency for smaller particles to merge until one large particle remains(Chun Zeng, 2007). To avoid aggregation, various stabilizers are used. A stabilizing agent assists in maintaining repulsive forces to overcome Wan der Vaal forces in the solution of NPs to prevent agglomeration. During the chemical synthesis of AuNPs, sodium borohydride or sodium hydride, sodium citrate, or ascorbic acid may act as capping and stabilizing agents for AuNPs. However, during the biological synthesis of AuNPs, stabilization of nanoparticles can be successfully achieved by using the bio-material rich in antioxidant properties. Gold nanoparticles are typically stabilized electrostatically where citrate-capped nanoparticles are negatively charged, and cetyltrimethylammonium bromide (CTAB)-coated nanoparticles are positively charged (Verma *et al.*, 2015).

For further application of metal nanoparticles, attaching the molecular recognition motifs (i.e. functional groups) of interest to the nanoparticle surface is of great importance. Most importantly, the functional groups should bind specifically to each other or to anything else present in the system under investigation. In addition, introducing multiple functionalities wouldbe of great value, as it provides more flexibility for multiplexing in analytical applications and new tools to control the bottom-up assembly of nanostructures.

2.4.8 Characterization of nanoparticles

2.4.8.1Transmission Electron Microscopy (TEM)

Transmission electron microscopy is the most useful imaging technique for nanoparticles. TEMS images allow researchers to view samples on a molecular level, making it possible to analyze structure and texture. An image is formed from the sample's electrons' interaction when a beam of electrons is transmitted through a sample. Owing to the smaller de Broglie wavelength of electrons, the instrument can capture fine detail (atomic resolution). Images are high-quality and detailed providing information of the surface

features, shape, size and structure of nanoparticles (Slistan-Grijalva *et al.,* 2005). This technique involves laborious sample preparation and the operation and analysis requires special training. Electron microscopes are sensitive to vibration and electromagnetic fields and must be housed in an area that isolates them from possible exposure. A Transmission Electron Microscope requires constant upkeep including, maintaining the voltage, current in the electromagnetic coils and cooling water (Choudhary *et al.,* 2018).

2.4.8.2 UV-vis absorption spectroscopy

The absorption of light by AuNPs can be measured by Uv-vis spectroscopy. When a beam of light of wavelengths in the visible and ultraviolet region passes through the specimen, itsintensity before and after interacting with a sample is measured to determine the light transmitted through or absorbed by the sample. The amount of light absorbed by the sample depends on the concentration, the path length of the light through the cuvette, and how well the analyte the light absorbs at a specific wavelength. Absorption peaks can also indicate the type ofbonds in a given molecule.

2.4.8.3 Scanning electron microscopy (SEM)

The sample's area to be analyzed is targeted by a narrowly focused electron beam that can be swept across the specimen's surface to form an image or target one place only to analyze a particular position. The image is produced due to the electron beam's interaction with atoms at or near the samples' surface. SEM can also produce very high-resolution images (1 to 5 nm) (Choudhary, 2017). Advantages of a Scanning Electron Microscope include its wide-array of applications, the detailed three-dimensional and topographical imaging and the versatile information garnered from different detectors. The disadvantages of a Scanning Electron Microscope start with the size and cost. SEMs are expensive, large and must be housed in an area free of any possible electric, magnetic or vibration interference. Special training is required to operate an SEM as well as prepare samples. In addition, SEMs are limited to solid, inorganic samples small enough to fit inside the vacuum chamber that can handle moderate vacuum pressure.

2.4.8.4 Dynamic light scattering (DLS)

DLS estimates the light scattered from a laser that passes through a colloid and particles' hydrodynamic size. DLS is also a non-invasive technique that requires comparatively low amounts of sample and provides reliable estimates of the quality of preparation rapidly (Sandhu *et al.,* 2018).

2.4.9 Mechanism of detection for *Ralstonia solanacearum*

Nano diagnostics involves nanotechnology in diagnosis to meet the demands for increased sensitivity and early detection in less time. The large surface area of nanomaterials enables the attachment of many target-specific molecules of interest for ultra-sensitive detection. With such capability, diagnosis at the molecular and single-cell level is possible. Because of high sensitivity, nanomaterials detect microorganisms or target molecular analytes specific to pathogens (Tallury *et al.,* 2010). Moreover, relatively small sample volumes are needed. NPs of various types have been primarily studied and have shown great promise for infectious plant diseases nano diagnostics. Given nanoparticles' specific physical and chemical properties, including AuNPs, these particles can be used as biological and chemical sensors to detectmaterial and analytes (Srivastava *et al.,* 2005). Bacterial pathogens are essential targets for detection and identification in various fields, including agriculture, medicine, food safety, public health, and security. Nano-biosensors offer a rapid and cost-effective method of bacterial detection, which can be used on-site without the need for specialized training, thereby preventing infection and decreasing disease spread. Colorimetric biosensors exploit analyte binding-induced changes in the sensor surface's optical properties (Ahmed *et al.,* 2014). Based on this knowledge, specific pathogens or materials produced by microbial pathogens can be easily detected using surface-functionalized gold nanoparticles. The surface chemistry of gold provides the ability to recognize bacteria or biomolecules produced by bacteria.

Bacteria located within the soil rhizosphere produce hormones such as auxins, gibberellins (GA), cytokinins, ethylene, and abscisic acid in *in-vitro* conditions (Patel *et al.*, 2015a). GAs are typical secondary metabolites in microorganisms; however, they act as endogenous hormones in higher organisms like plants (Sharma *et al.*, 2018). There is no known role for gibberellin production in bacteria; instead, they seem to be secondary metabolites that may be signaling factors towards the host plant (Bottini *et al.*, 2004). Bacterial phytohormones are produced, excreted, and transferred in plant cells during plant–bacterial interaction.

Gibberellins are complex organic molecules chemically known as tetracyclic di-terpenoid acids having the molecular formula $C_{19}H_{22}O_6$ (Silpa *et al.*, 2018). Many gibberellins have been defined using modern analytical techniques, and 126 GAs have been identified in plants, fungi, and bacteria (Gomi & Matsuoka, 2003). Gibberellic acid (GA_3) is the main product of gibberellins in fungi and bacteria (Brückner & Blechschmidt, 1991). For example, about 20 different types of gibberellins are produced by *Gibberella fujikuori*, of which GA_3 is most abundant (Patel *et al.*, 2015b). The functionalized surface of NPs provides a convenient scaffold to attach GA_3, produced by *Ralstonia solancaerum* which is expected to facilitate detection of bacterial wilt. In the presence of GA-mediated *R.solanacearum*, the absorption band may shift due to aggregation or dispersion accompanied with a visible colour change in the NP solution observable with the "naked eyes" which is expected to confirm the pathogen's presence as illustrated in Figure 2 below.

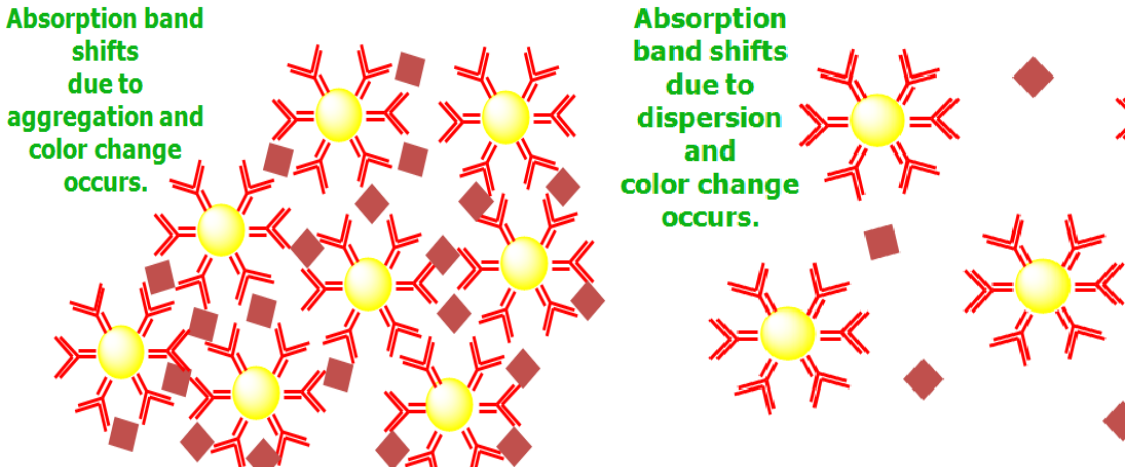

Figure 2.5: Aggregation and Dispersion of nanoparticles.

2.4.10 Characterization of Biomolecules

2.4.10.1 High-Performance Liquid Chromatography (HPLC)

High-Performance Liquid Chromatography (HPLC) is a sensitive and precise method used to identify, quantify, and purify a sample's components. The specific intermolecular interactions between the molecules of a sample and the packing material define their time on-column." Hence, different constituents of a sample are eluted at different times. Thereby, the separation of the sample ingredients is achieved. HPLC is a routine procedure in the purification and separation of gibberellins. High-performance liquid chromatography offers a fast and precise quantitative analysis. It is highly reproducible and manages all areas of analysis to increase productivity. The HPLC is very rapid, efficient, and delivers high resolution as compared to other chromatographic techniques, such as TLC, column chromatography, and paper chromatography. However, the HPLC pump process reliability relies on of cleanliness of the sample, mobile phase, and proper operation of the system. The separation in High-performance liquid chromatography has less efficiency than gas chromatography.

2.4.10.2 Fourier transform infrared spectroscopy (FT-IR)

Fourier Transform Infrared Spectroscopy (FT-IR) identifies chemical bonds in a molecule or detects different functional groups by producing an infrared absorption spectrum. The sample's reflectance and transmittance of the infrared rays at different frequencies are translated into an IRabsorption plot consisting of reverse peaks. It is a non-destructive and high resolution technique in which both organic compounds and inorganic compounds can be easily identified. This spectroscopy gives better signal to noise ratio compared to the dispersive instruments. The main disadvantage of this method is the FTIR instrument has only a single beam while, dispersive instruments generally have a double beams.

CHAPTER THREE

MATERIALS AND METHODS

3.1 Overview/Introduction

This chapter presents the experimental aspects of this study. It provides details of the general reagents and equipment used as well as the experimental procedures for the three objectives of the research work, i.e. i) Development of a gold nanoparticle-based colorimetric probe, (ii) Determining colorimetric probe sensing mechanism of *Ralstonia solanacearum* mediated exudates, (iii) Efficacy of colorimetric probe for rapid detection of *R.solanacearum.*

3.2 Research site

The study was conducted under laboratory and greenhouse conditions at Jomo Kenyatta University of Agriculture and Technology (JKUAT) in Juja, Kiambu County.

3.3 General materials, reagents and preparation of stock solutions

All chemicals (as hereby listed) were of analytical grade and were obtained from Fisher Scientific, UK and Loba Chemie Pvt Ltd: Chloroauric acid (ACS reagent ≥ 49.0, Au basis $HAuCl_4.H_20$, MW = 357.8018g/mol),tri-Sodium citrate dehydrate ($C_6H_5Na_3O_7.2H_2O$, MW = 294.09g/mol, 99%) and sodium chloride (NaCl, MW = 58.44g/mol). Gibberellins, Ethanol, Diethyl ether, Ethyl acetate were of analytical grade and were used as obtained from Sigma Aldrich (St. Louis, MO USA). Acetonitrile was of HPLC grade procured from Merck India Ltd. All experimental manipulations and data collection were performed at room temperature (21°C) unless otherwise stated. Standard solutions were freshly prepared by dissolving known quantities of Gibberellic acid in deionized water.

3.4 Instrumentation and measurements

The synthesized AuNPs were characterized using Transmission Electron Microscope (TEM), Scanning electron microscopy (SEM), Dynamic light scattering **(**DLS), and Uv-vis spectroscopy. This study used characterization techniques to confirm products' successful formation and morphology after synthesis and to study the optical properties of the developed colorimetric probe.

This study determined the size and shape of AuNPs using a scanning electron microscope FEI XL30 Sirion FEG (Oxford Instruments Plc,Abingdon, United Kingdom). The system was equipped with an Energy Dispersive X-ray Spectrometer (EDS) system from EDAX, having a lithium doped silicon detector operated at an accelerating voltage of 30 kV. Samples for SEM observation were prepared by mounting AuNPs on specimen stubs and then coating them with gold in a sputter coater device. Electronic absorption spectra were recorded on a Shimadzu (Shimadzu Japan) UV/VIS 1800 spectrophotometer in the region between 300- 800nm.

3.5 Development of a colorimetric probe using gold nanoparticles

3.5.1 Preparation of gold nanoparticles (AuNPs) using the citrate reduction method

The gold nanoparticles (AuNPs) were synthesized following the citrate reduction method, as described by Tyagi *et al.,* 2016, with customized modifications to meet the specifications of the targeted probe. Using 10% w/v HNO_3, all glassware was cleaned and rinsed thoroughly with distilled water. All other solutions were prepared using deionized water. The synthesis of AuNPs was conducted as follows: Chlorauric acid ($HAuCl_4$) was heated to boiling. An aqueous solution of 1% trisodium citrate was quickly added to the solution. The solution in the beaker was boiled on a hot plate until the temperature reached 97^0C under rapid magnetic stirring. The reaction was run until it reached a wine-red colour, indicating its end. This solution was cooled naturally to room temperature and stored at 4°C in a dark coloured glass bottle before use.

3.5.2 Optimization of reaction conditions during the synthesis of AuNPs

The pH of the reaction mixture, temperature, and reaction time during the synthesis of AuNPs was optimized while measuring the absorbance spectra on UV/VIS. Ten ml aliquots of the formed AuNPs suspension were added into 5 test tubes. The suspensions in the test tubes were then subjected to different pH conditions ranging from pH 2.5-11.5. The specific pH conditions tested were pH 2.5, 3.5, 4.5, 6.5 and 11.5. The pH was adjusted by either adding drops of 1 N NaOH or 1 N HCl until the desired pH was achieved while observing the pH meter. Varying temperature and reaction periods were studied by subjecting 10ml of the AuNPs solution in boiling tubes to different temperature conditions by heating in a digital water bath for 3 min each and measuring the absorbance spectra on the UV/VIS in a scan range of 300 nm to 800 nm. The varied temperatures included 50°C, 60°C, 70°C, 80°C and 90°C. The UV/VIS spectra were standardized by plotting graphs of absorbance against wavelength.

3.5.3 Characterization of AuNPs

The synthesized AuNPs were characterized using Transmission electron microscopy (TEM), scanning electron microscopy (SEM), Dynamic light scattering (DLS), and Uv-vis spectroscopy. Using TEM, gold nanoparticles were visualized on a Tecnai G2 Spirit (Thermo Fisher Scientific, Oregon USA) operated at 120 kV. Ten microliters of the colloidal sample were placed on a carbon-coated copper grid and dried at room temperature (Electron microscopy science, CF300- CU). The size and shape of AuNPs were determined using a scanning electron microscope FEI XL30 Sirion FEG (Oxford Instruments Plc, Abingdon, United Kingdom). The system was equipped with an Energy Dispersive x-ray Spectrometer (EDS) system from EDAX, having a lithium doped silicon detector operated at an accelerating voltage of 30 kV. Samples for SEM observation were prepared by mounting AuNPs on specimen stubs and then coating them with gold in a sputter coater device. Electronic absorption spectra were recorded on a Shimadzu (Shimadzu Japan) UV/VIS 1800 spectrophotometer in the region between 300-800nm. Samples were prepared in 1ml cuvettes before analysis. Dynamic light scattering (DLS) was carried out

on a DAWN Enhanced Optical System (DAWN EOS, Wyatt Technology Corporation). Zeta potential measurements were operated on a Nano- ZS instrument, model ZEN 3600 (Malvern Instruments).

3.5.4 Sensitivity studies

To demonstrate the principle behind the assay, it was first determined whether synthetic gibberellic acid could cause aggregation or dispersion of the synthesized AuNPs. Therefore, a typical experiment was conducted to assess the sensitivity of the developed colorimetric probe. Standard solutions of synthetic gibberellic acid (GA_3) were prepared by appropriate dilution of the stock solution with double-distilled deionized water at varying concentrations 0.1-1.0 ppm. GA_3 is the main product of gibberellins in fungi and bacteria. It is also a terpenoid hormone that is an important phytohormone regulating plant growth and development The GA_3 solution was added to 1800µl of AuNPs solution (Jongjinakool*et al.*, 2014), and the resultant mixture was monitored for observable colour change.

3.6 Quantification of Gibberellic acid

3.6.1 Soil and plant sampling

The sampling was conducted in Kajiado, Kiambu, Bomet, and Kirinyaga counties in Kenya. These counties have been reported to experience economically significant crop losses in tomatoes due to the bacterial wilt disease (Ireri*et al.*, 2018; Karuku *et al.*, 2017). Soil samples (100g) were randomly collected from the rhizosphere of tomato plants, exhibiting bacterial wilt symptoms. A sterile auger collected the soil samples by digging vertically underground 10-20 inches deep. The soil samples were pooled to constitute a single sample and transported to the JKUAT laboratory for analysis. The samples were stored in a refrigerator set at 4°C for further studies.

3.6.2 Isolation of *Ralstonia solanacearum*

Soil samples (10g) were aseptically transferred into 250 ml conical flasks containing 90 ml of sterile water. The suspension was homogenized by shaking on a rotary shaker for 10 minutes to dislodge the soil colloids' bacterial cells. The samples were serially diluted (by a 10^{-3} dilution factor), and 10 µL and 20 µL of the bacterial suspension were spread on plates containing CPG media amended with TZC. The bacterial cultures were incubated at 28°C±2°C overnight in an upside-down to allow bacteria growth for 48h, and virulent colonies of *R.solanacearum were* identified by their large and elevated size, fluidal nature, and colour. Mutant or non-virulent colonies of *R. solanacearum* are uniformly round and dark red, smaller in size and butyrous (Peeters *et al.,* 2013).

3.6.3 Extraction of Gibberellins

Colonies of *R.solanacearum* exhibiting virulent characteristics were selected and streaked using a sterile loop onto 1L flasks containing 500 ml Nutrient Broth media (N.B.). The culture was grown on a rotary shaker at 28±2°C with shaking at 200 × g for 24h for GA_3 production. After removing the bacterial cells by centrifugation, the supernatant was reduced to 50ml by evaporation under vacuum and extracted with ethyl acetate. Gibberellic acid was extracted using ethyl acetate and $NaHCO_3$ in a ratio of 1:3 according to the protocol by (Patel *et al.,* 2015b). The extracts were filtered through 0.45µm membrane filters and chromatographed using HPLC to determine quantity of GA_3 present in the bacterial isolates.

3.6.4 Quantification of GA_3 isolated from *Ralstonia solanacearum* isolated from soil samples using High-Performance Liquid Chromatography (HPLC)

A reverse phase HPLC technique was used for the quantitative analysis of gibberellins. The stationary phase consisted of LiChrospher on the RP-18 packed stainless- steel column (250 x 4 mm i.d.). The chromatograms were recorded on an NT-based Chemstation program. Acetonitrile and acidic water (60:40 v/v in 0.01 % H_3PO_4) were used as the mobile phase with a flow rate of 0.5 ml min^{-1}. Synthetic Gibberellic acid (GA_3) was

used as the standard. Standard solutions of the GA_3 were prepared by dissolving 50 mg of GA_3 in 10ml acetonitrile. Working standards of 0.1-1.0 ppm were serially diluted, and 20 µL of each standard concentration was injected in HPLC set at a wavelength of 206 nm. After standardization, 20 aliquots of GA_3 extracted from *R. solanacearum* were injected in HPLC set under the same conditions. Each run was repeated three times, and detector response was measured in peak area to standardize the analysis method to obtain a separate sharp peak for each analyte. The quantity of gibberellins present in the microbial filtrate extract was calculated using the following equation (Bhalla *et al.*, 2010):

$$y = \frac{\alpha \times c \times v}{\beta}$$

Where γ is the concentration of the desired analyte (as indicated by HPLC retention time) in the sample (µgg−1); α is the respective peak area of sample aliquot; β is the peak area of the respective standard; c is the concentration of the standard solution (µgml−1); v is the volume made for sample extract.

3.6.5 FT-IR analysis of GA_3-mediated *Ralstonia solanacearum*

FT-IR spectra of GA_3 were recorded using a Shimadzu 8400 Fourier Infrared spectrophotometer (Shimadzu, Japan). Gibberellins were extracted and separated from the supernatant as described in section 3.6.3. The extracted GA_3samples were spotted on KBr discs. The samples wereanalyzed between the scanning range from 400 to 4000 cm^{-1}. The presence of gibberellins in the isolate was confirmed using FT-IR. The FT-IR of extracted GA_3 were compared with the standard spectrum of GA_3.

3.6.6 Real sample analysis

The proposed method was used to detect GA_3 in soil samples from different counties in Kenya. Detection of the presence of GA_3-mediated *R. solanacearum* using AuNPs was evaluated using UV-vis spectroscopy. Bacterial wilt infected soils from Kajiado, Kirinyanga, Bomet and Kiambu counties were used. A predetermined volume of bacterial wilt-infected soils (0.5g) was added to 1800µl of the colloidal solution.

3.7 Determination of efficacy of developed probe under *in-vitro* conditions

3.7.1 Experimental design

The *in-vitro* experiment under greenhouse conditions followed a Completely Randomized Design (CRD). Tomato seedlings were inoculated with *R. solanacearum* at varying inoculum density (10^8 CFU/ml, *i.e.*, level known to cause bacterial wilt (Vailleau *et al.*, 2007), 10^6 CFU/ml, 10^4 CFU/ml) and non-inoculated plants (negative control). Each assay was replicated three times, with 16 plants per treatment.

3.7.2 Greenhouse assay

Tomato seedlings of the cultivar Rio Grande were raised under greenhouse conditions at 25°Cfor 2-3 weeks before inoculation in sterile pathogen-free peat moss. Three-week-old healthy plants were inoculated with *R.solanacearum* at 10^8 CFU/ml, 10^6 CFU/ml, and 10^4 CFU/ml inoculum density by soil soak inoculation. Inoculation was performed by pouring 20 ml of the bacterial suspension onto the soil at the plant base. Before inoculation, roots were wounded using a sterile spatula, and for the negative control, plants were treated with a saline solution.

Disease development was evaluated daily, and typical symptoms of bacterial wilt appeared five days after inoculation. Symptoms observed in infected tomatoes were wilting during the hottest part of the day. Initial wilt symptoms appeared on the leaves and progressed with time after inoculation. Wilt symptom development was assessed and recorded using

an ordinal disease index scale (Winstead & Kelman, 1952) ranging from 0 (no wilting symptoms) to 4 (all leaves wilted) for up to 15 days after inoculation. Re-isolation of bacteria onto the Casamino- acid Peptone-Glucose (CPG) medium with TZC from the vascular tissue of inoculated and non- inoculated control plants was done. Identification of re-isolated pathogen was carried out morphologically according to (Buddenhagen & Kelman, 1982.).

3.8 Statistical analysis

All the data obtained in this study were recorded in Excel and then subjected to a One-way Analysis of Variance (ANOVA) using GenStat® statistical program, 17th edition (GenStat, 2017). Treatment means were separated using Tukey's HSD (honestly significant difference) test at $P < 0.05$

CHAPTER FOUR

RESULTS AND DISCUSSION

4.1 Development of colorimetric probe using gold nanoparticles

Colour changes were observed in the reaction mixture when 1200µl of trisodium citrate solution was added into 500 ml of HAuCl4 solution. The solution colour changed rapidly from pale yellow (Fig. 4.1A) to dark blue (Fig. 4.1B) and finally to wine-red (Fig. 4.1C). These changes were observed within a 10 minutes reaction time. These colour changes are characteristic of the formation of AuNPs bycitrate reduction of auric acid and were in accordance with previous studies (Bast *et al.*, 2011; Faramarzi & Forootanfar, 2011; Verma *et al.*, 2014). The yellowish Au^{3+} solution turned dark blue and finally wine-red, which indicated the existence of AuNPs in the solution. This finding agrees with similar studies in which the citrate reduction method was used to develop AuNPs with a wine-red colour (Figure 4.2 inset) (Faramarzi & Forootanfar, 2011; Ngumbi *et al.*, 2018). The presence of AuNPs in the resulting solution was established based on characteristic colour, which involves light absorption within the visible spectrum. Gold nanoparticles' properties differ from their bulk form because bulk gold is yellow solid and inert, while gold nanoparticles are wine-red/ red (Rashid *et al.*,2014). Additionally, AuNPs are red in colloidal solutions because of the Mie absorption by their surface plasmon oscillation that peaks at 520 nm (Figure 4.2) (Guieu *et al.*, 2011).

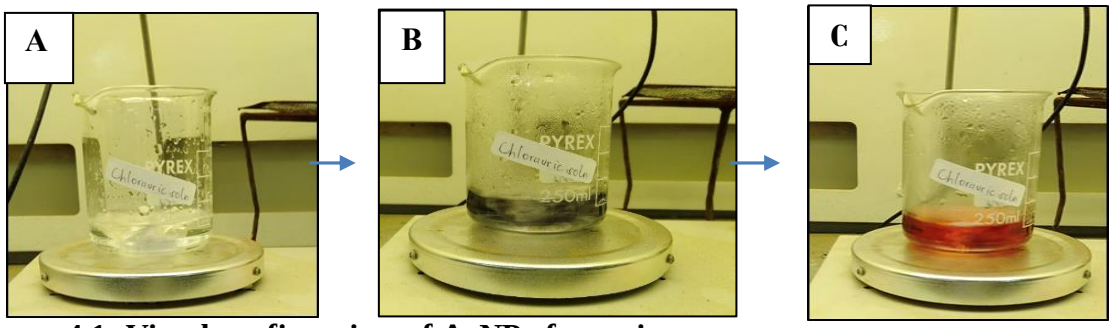

Figure 4.1: Visual confirmation of AuNPs formation

The results of the synthesis reaction conform to the reduction process summarized by Verma *et al.,* 2014 as:

$2HAuCl_4 + 3C_6H_8O_7$(citrate) $\rightarrow 2Au + 3C_5H_6O_5$ (3-ketoglutaric acid) $+ 8HCl + 3CO_2$

Kumar *et al.,* 2007 proposed that Au^{3+} is reduced to Au^{+} by the oxidation of trisodium citrate to dicarboxyacetone. Gold atoms are formed when Au^{+} undergoes disproportionation, which is alsocatalyzed by the gold surface. The colloidal solution retained a red colour indicating successful stabilization of the gold nanoparticles using citrate ions up to a month when stored in a dark colored glass container. Citrate anions have been reported to reduce gold ions to atoms and stabilize colloidal AuNPs (Park & Shumaker-parry, 2020). The citrate ions act as a reducing agent for Au ions and as a stabilizing agent by forming a layer over the nanoparticle surface, preventing aggregation or agglomeration of AuNPs. The citrate ionlayer protects the nanoparticles from van der Waal-induced aggregation via electrostatic repulsion and renders them soluble in water. When using trisodium citrate, very narrow size distributions of highly spherical particles can be achieved with a standard deviation of less than 10% (Kumar, 2012). Stabilization also restricts the nanoparticle growth to a critical size (5nm-50nm), and hence, the nanoparticles are more stable. This was evidenced by the stable retention of the solution colour in this study. Citrate-stabilized AuNPs have successfully been used as tunable foundational materials for a wide range of AuNP-based interfacial studies and applications, including nanoparticle assembly, particle aggregation, surface charge, particle growth mechanisms etc. (Park & Shumaker-parry, 2020).

In a preliminary experiment, a synthetic gibberellic acid (GA_3) stock solution was prepared in a 100 ml volumetric flask with deionized water. An aliquot (1mL) of the stock solution was measured in a sample vial, 1,800µl of AuNPs solution and the resulting mixtures were then allowed to react for 3 min. The mixtures were directly used in the spectroscopic measurement. Optical absorption spectra were taken in the wavelength range 300–800 nm at room temperature using a quartz cell (Tyagi *et al.,* 2016).

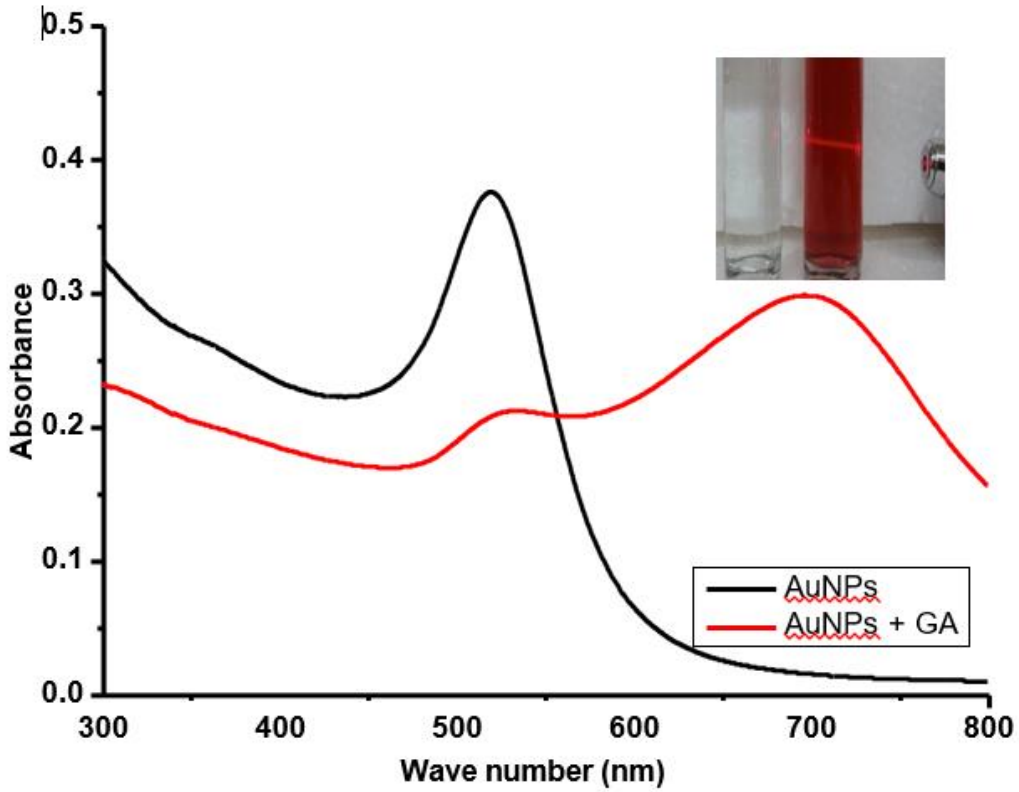

Figure 4.2: Absorption spectra of AuNPs dispersed in aqueous solution before and after the addition of Gibberellic Acid. Inset: Tyndall scattering effect under a *632.8nm laser beam*

The freshly synthesized AuNPs were found to have a sharp surface plasma resonance peak at about 520 nm (Figure 4.2) compared to the suspension containing synthetic GA. Previous studies conducted by Faramarzi & Forootanfar, 2011indicated similar results. The absorption spectra of the gold solution indicated the formation of gold nanoparticles due to the presence of the SPR maxima of the AuNPs at 520 nm. For well-separated AuNPs in an aqueous environment, the resonant condition is satisfied at around 520 nm, giving a distinctive red colour to the solution of these particles (Alex & Tiwari, 2015),which also indicates the generation of AuNPs of small size (Pienpinijtham *et al.*, 2012).

A laser beam shone through a transparent glass bottle containing the freshly synthesized AuNPs solution, illustrated the Tyndall effect. The presence of individual particles that are large enough to scatter and reflect light in the direction of the observer's eye made the beam visible (Tyndall effect), as shown in Figure. 4.2 inset. If a beam of converging rays (with the wavelength of 630–680 nm) passes through a liquid containing minute particles in suspension, each of these particlesscatters the light rays that fall on it, and it becomes a luminous point. Thus, the rays' entire path through the liquid becomes visible (Pang *et al.*,2012). The Tyndall effect, which comes fromlight scattering by particles in a colloid or a fine suspension, is used to confirm the nanoparticles' existence in nanofluids. This phenomenon does not occur in true solutions, e.g. water. Tyndall effect indicates the presence of nanoparticles in a colloidal solution that absorbs light within the plasmonic frequency range (Tyagi *et al.*, 2016). This gold nanoparticle solution was found to be stable for about one month showing no precipitation or colour change

4.2 Optimization of reaction conditions during the synthesis of AuNPs

Gold nanoparticles exhibit SPR, which allows the absorption and scattering of incident radiation that can be measured using UV–Vis spectrophotometry. The SPR band intensity and wavelength are dependent on particle properties such as the shape, structure, metal type, size, and dielectric material surrounding the medium (Gavamukulya *et al.*, 2020). The effect of different reaction conditions (temperature, reaction time and pH) were monitored.

4.2.1 Temperature

Figure 4.3 illustrates the effect of temperature on AuNPs suspensions determined by UV/Vis spectroscopy. Changes in surface plasmon resonance (SPR) peaks were observed with varying temperature conditions until a maximum peak was attained. As the suspension temperature was increased from 50 to 90°C, a hypsochromic shift was observed in the nanoparticles' UV spectra (Figure 4.3). It was evident that at all tested temperatures, the AuNPs remained stable, maintaining a characteristic absorption maximum of between 520 nm to 530 nm, which was within the AuNPs range (500-600nm). Gavamukulya *et al.*, 2020

illustrated in a similar study the effect of temperature stability on silver nanoparticles remaining stable with increasing temperature up to 85°C while maintaining a characteristic absorption maximum of between 420nm to 530nm.

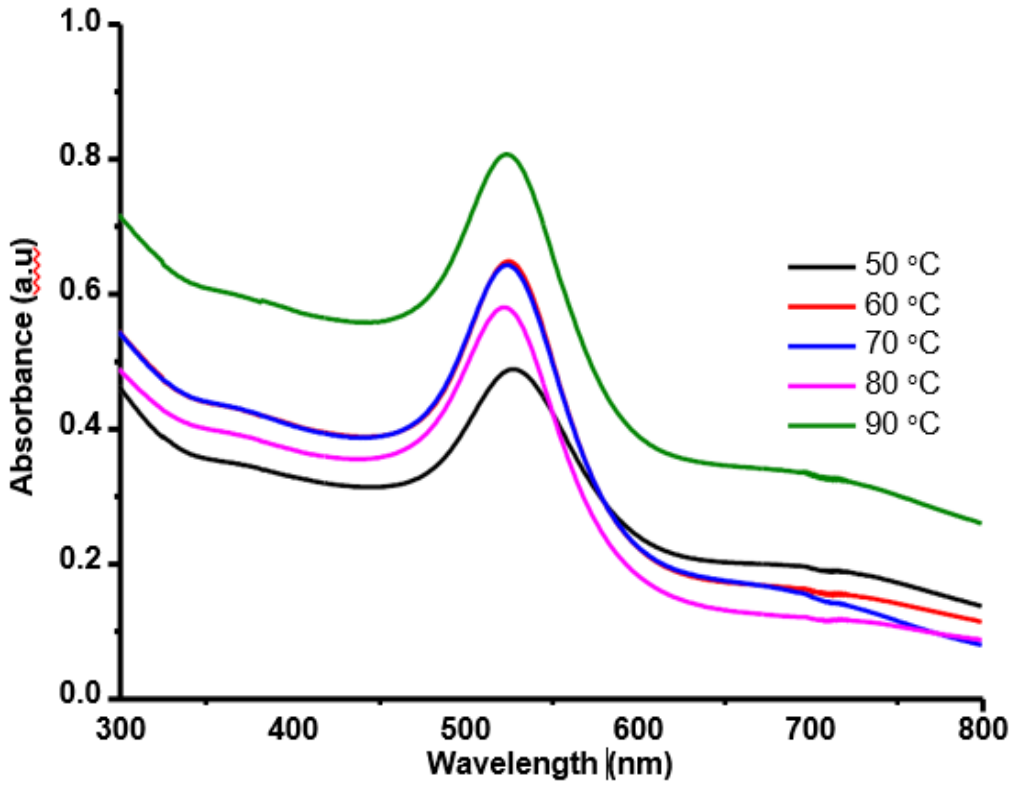

Figure 4.3: Absorption spectra of AuNPs synthesized at different temperature

4.2.2 Reaction time

The absorbance spectra of the AuNP suspensions were measured on the UV/VIS spectroscopy ina scan range of 300 nm to 800 nm. Changes in surface plasmon resonance (SPR) peaks were alsoobserved with varying reaction times. SPR peaks increased with increasing reaction time until a maximum peak was attained (Fig. 4.4).

Bathochromic shifts developed between 0-4minutes of the reaction. The absorbance value of the band increased with increasing time indicates that the continued reduction of metal ions and concentration of nanoparticles increased. The formation of AuNPs started within 6 min, and then the intensity of the SPR peak increased up to 22min. After that, no substantial change in the SPR peak was observed. These findings corroborate studies conducted by Bindhu & Umadevi, 2014. As the effect of reaction time, the SPR bands of the prepared AuNPs exhibited a blue shift (550– 546 nm) with increasing absorbance. Further, the formation of AuNPs began within 10 min, and the intensity of the SPR peak continued to increase up to 6 h. This stability may have resulted from a potential barrier due to the competition between weak Van der Waals forces of attractionand electrostatic repulsion.

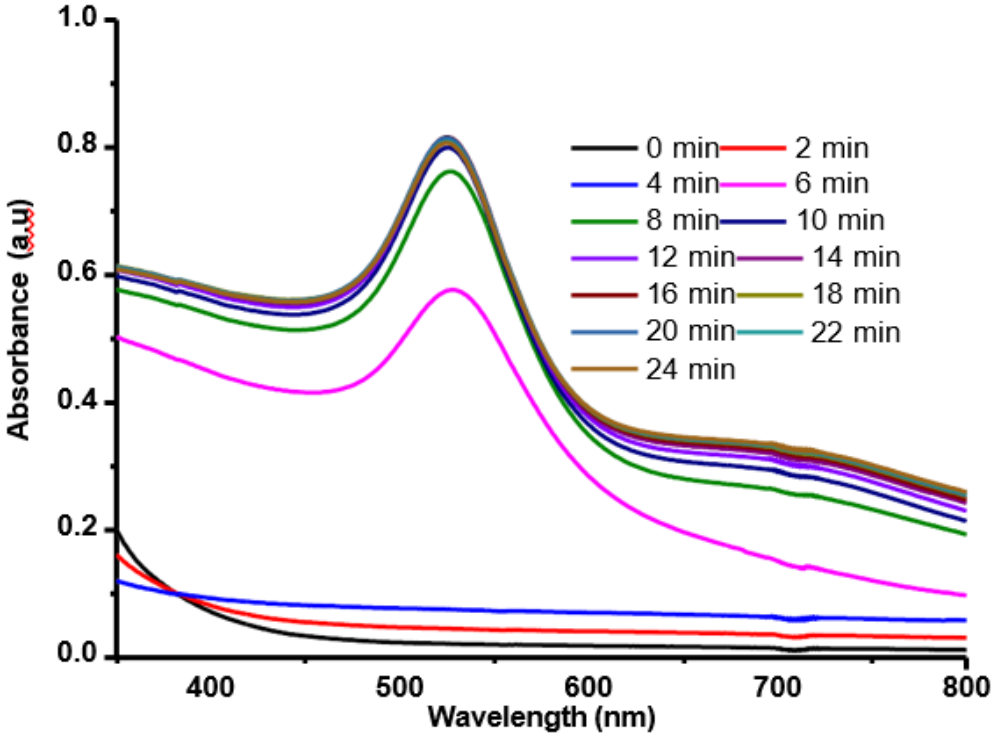

Figure 4.4: Absorption spectra of AuNPs synthesized at different reaction times

4.2.3 pH

Reaction mixture pH plays a vital role in the size and shape control of the gold nanoparticles. Figure 4.5 illustrates the pH effect on AuNPs suspension as determined by UV/Vis spectroscopy.No defined absorption peaks were observed when the reaction's mixture pH was adjusted to between 2.5 and 3.5 (acidic conditions) (Figure 4.5). The absence of the SPR peaks impliesthat the synthesis of AuNPs did not occur at these particular pH values. However, SPR peaks were observed when the pH was adjusted to 6.5 and 11, indicating that the synthesis of AuNPs was appropriate between these pH values. However, at extremely high alkaline conditions, AuNPs rapidly aggregated and precipitated in agreement with results obtained by Pienpinijtham *et al.*, 2012. A characteristic wine-red and an absorption band centered at 520 nm further confirm AuNPs synthesis's presence at pH values 6.5 and 11. As mentioned previously, the macroscale, the element of gold, is gold-coloured. However, the gold element is purple to red at the nanoscale, resulting from scattering a light beam upon interacting with particles in a colloidal solution. Therefore, the formation of gold nanoparticles can be observed by a change in colour.

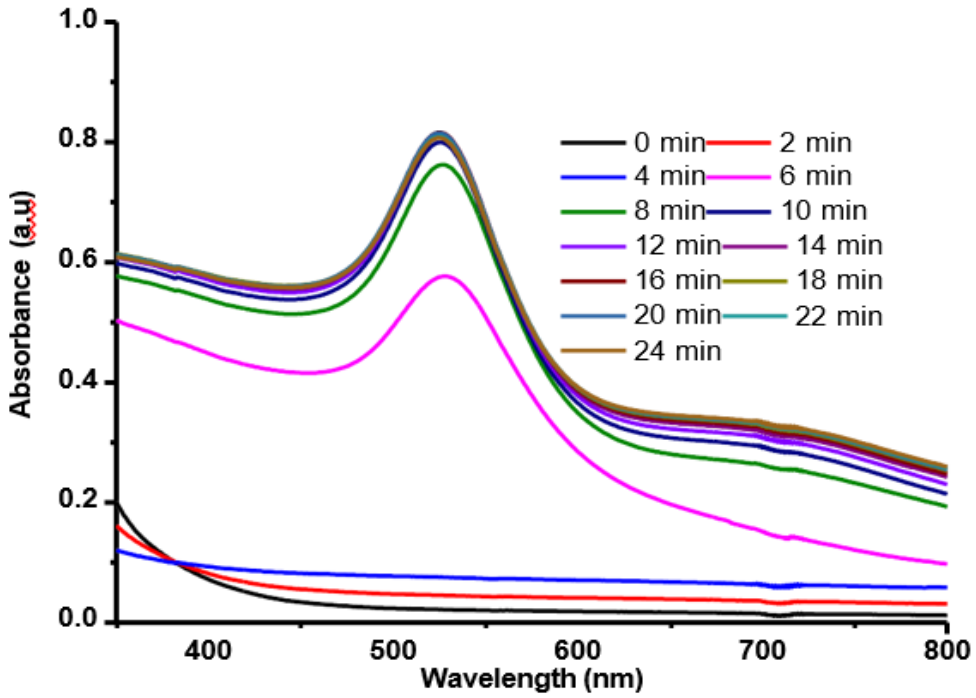

Figure 4.5: Absorption spectra of AuNPs synthesized at various pH values

4.3 Characterization of AuNPs

The optical characterization of the synthesized AuNPs was carried out using UV-visible spectroscopy. The size and morphology of AuNPs were observed using Dynamic light scattering (DLS) and SEM. In TEM, each sample's particle size and size distribution were obtained by Fiji image analysis.UV-visible spectrum

UV-Vis spectrophotometry (300-800 nm at room temperature) was used to confirm the fabrication of spherical AuNPs. The aqueous dispersions of AuNPs showed the typical SPR bandat 520nm in the UV-vis spectrum (Figure 4.2), in accordance with the values observed for dispersed AuNPs with sizes smaller than 25nm (Haiss *et al.*, 2007; Lin *et al.*, 2004). A strong resonance is seen and arises due to the excitation of surface plasmon vibrations in the gold nanoparticles. AuNPs generally show absorption peaks from 500 to 550 nm, redshifting with an increase in particle size, giving red-coloured solution with particles

smaller than 90 nm and purple or blue colour for higher particles (Alex & Tiwari, 2015). There was a colour change of the AuNPs solution from wine-red to purple, followed by shifting the SPR peak to a longer wavelength region (716 nm), which indicated the probability of the successful conjugation of AuNPs by GA_3.

4.3.1 Dynamic light scattering

Dynamic light scattering (DLS) results showed that the average hydrodynamic diameters of the synthesized particles were in the range of 30-40 nm (Figure.4.6). DLS measurements record higher values since light is scattered by the core particle and the layers formed on the particle's surface. The zeta potential of synthesized AuNPs was found to be -0.57±0.48 Mv. Their surface charge influences the stability of the dispersed particles. Zeta potential is used as the index of thesurface charge of the particles. If the zeta potential is high, the particles are deemed stable due to the high electrostatic repulsion force between particles. On the contrary, the probability ofparticle collision becomes high, resulting in particle aggregation when zeta potential gets close to zero (Pang *et al.*, 2012).

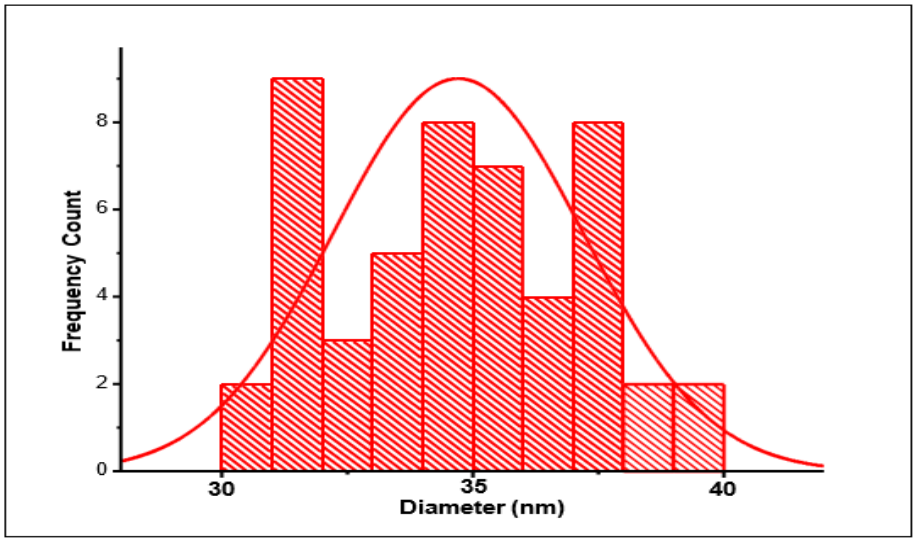

Figure 4.6: Hydrodynamic diameters of AuNPs as determined by dynamic light scattering

4.3.2 SEM andTEM characterization

The AuNPs were dispersed, as shown in SEM micrographs (Figure 4.7A inset). The nanoparticles' dispersed nature was further confirmed by the TEM micrographs (Figure 4.7B inset). Differences in the size of NPs can be attributed to varying reaction conditions. An assumption is made that an adsorbing layer of citrate anions on the NPs surface preventsagglomeration. The obtained colloidal solution was very stable and did not show any precipitate for at least one month without adding any organic stabilizer, implying that citrate served both asa reductant and an efficient stabilizer. This stability is important for the probe hosted in solution and furthers the successful generation of analyte induced colour signals (Vilela *et al.*, 2012; Zhao*et al.*, 2008).

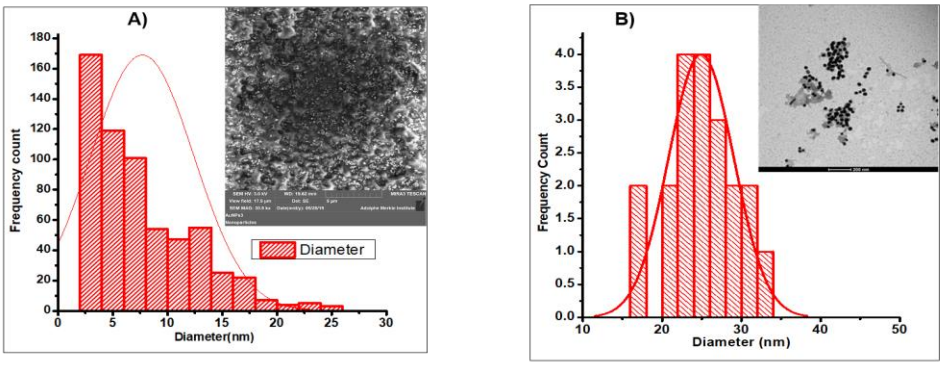

Figure 4.7: Size distribution of AuNPs determined by A) Diameter as determined by SEM, inset (SEM micrograph) B) Diameter as determined by TEM, inset (TEM micrograph)

The TEM image shows gold colloid in a monodispersed state because of the negatively charged layer of citrate ions, which repel each other. The diameters of the synthesized nanoparticles determined by TEM were found to have values ranging between 15 to 30 nm (Figure 4.7B). Ngumbi *et al.*, 2018, in a similar study, investigated the influence of different parameters on the size and morphology of AuNPs using citrate reduction. Both studies indicate that the growth of AuNPs was not homogeneous since the rate of growth

was determined by the relation between the diameter of the growing particle and the quantity of gold added.

4.4 Sensitivity studies

Figure 2.2 illustrates the principle behind the colorimetric probe sensing mechanism based on the aggregation of AuNPs. Varying concentrations of GA_3(0.1ppm-1.0ppm) were added to the AuNPs dispersion, and the colour changed from wine–red to blue to purple (Figure 4.8 Inset). AuNPs in solution are usually dispersed due to the adsorbed negative ions on the NP surface. The repulsion caused by the ions prevents the strong van der Waals attraction between gold particles from forcing them to agglomerate. In the absence of GA_3, AuNPs were dispersed in solution. As shown in Fig. 4.2, the characteristic plasmon resonance peak of dispersed AuNPs was at 520 nm.

The peak intensity at 520 nm became weaker with increasing GA concentration as new SPRbands appeared (Figure 4.8).

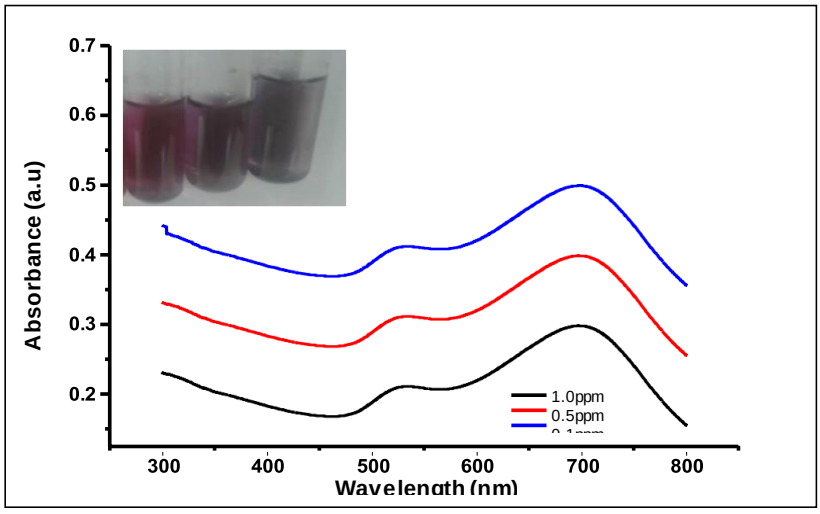

Figure 4.8: U.V.–vis spectra obtained from adding the GA at 0.1 ppm, 0.5 ppm, 1.0 ppm (left to right) into AuNPs solution. Inset: Visual colour change

A shift in the SPR band to a longer wavelength of ~700 nm (Figure 4.8) occurred with each concentration of GA_3 with a concomitant change in colour to purple, as shown in Fig 4.8 inset. Asimilar study of gold ion reduction by citrate ions reported that citrate functions as a reducing agent and a stabilizer that prevents the nanoparticles from aggregating (J. Park & Shumaker- parry, 2020) and, further, broadening of SPR bands. A previous study conducted by Raj *et al.*, 2015 also illustrated that the aggregation of cysteine gold nanoparticles (CAuNPs) in *Escherichia coli* bacteria in urinary tract infection (UTI) patients resulted in the broadening of spectra. The significant advantage of the AuNPs-based colorimetric assay is that the molecular recognition event can be transformed into colour changes, which the "naked eyes can easily observe"(Zhao *et al.*, 2008).

4.5 Quantification of GA_3 using HPLC analysis

Ralstonia solanacearum produce GA_3in culture extract that can easily be detected using HPLC (Karadeniz *et al.*, 2006). As shown in (Fig. 4.9), the calibration curve was used to calculate the quantity of GA_3 from each *R.solanacearum* concentration.

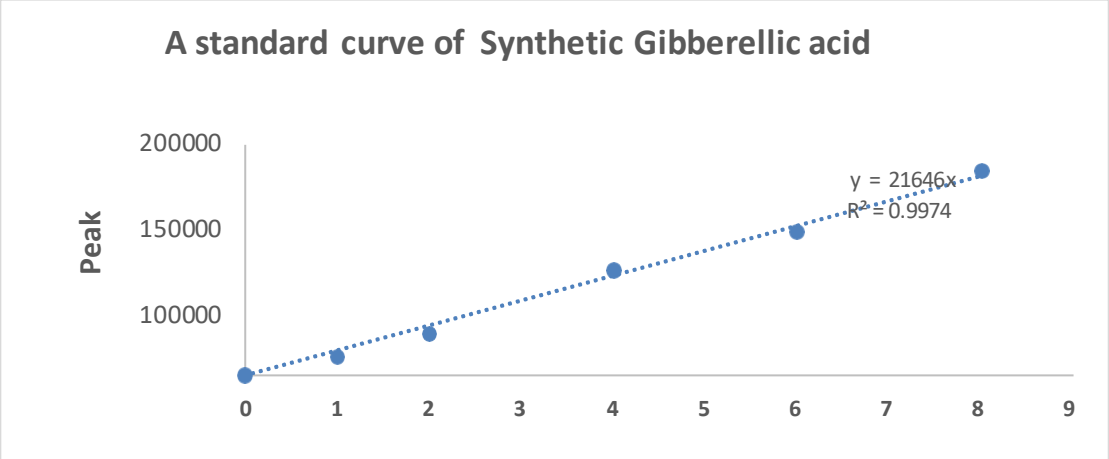

Figure 4.9: A standard curve of synthetic gibberellic acid obtained after injection into HPLC set

Significantly ($p \leq 0.05$) varying concentrations of GA_3(83.487µg, 42.543µg, and 31.672µg) were obtained from *R. solanacearum* inoculum densities of 10^8, $10^{6,}$ and 10^4 CFU/ml respectively (Table 4.1).

Table 4.1: Peak Height and Peak areas of GA3 extracted from R.solanacearum isolates asdetermined by HPLC

Ralstonia concentration (CFU/ml)	**% Area**	**Retentiontime**	**Peak height**	**GA_3 concentration (µg/100g)**
1x10 ^{4}	0.51	6.257	3873	31.672 b
1x10 ^{6}	0.6	6.297	4927	42.543 b
1x10 ^{8}	1.3	6.261	10913	83.487 a

Values within columns followed by the same letter are not significantly different at $p \leq 0.05$

Increasing GA_3 concentration was observed with increasing *R. solanacearum* inoculum strength. The 10^8 CFU/ml incolum density produced a quantity of GA_3 significantly different from the 10^4 and 10^6 CFU/ml inoculum density. In similar studies, isolates of fluorescent *Pseudomonas sp* were observed to produce gibberellins ranging from 419-485.8µg/ml (Bhalla *et al.*, 2010). Gibberellins from 28 strains of *Fusarium* were also quantified and classified as low, moderate and high producing as reported by Sharma *et al.*, 2018. These results further corroborate our study findings.

4.6 FT-IR spectra of GA_3-mediated *Ralstonia solanacearum*

The FT-IR spectra of GA_3 extracted from *R. solanacearum* were compared with standard gibberellic acid, as illustrated in Figure. 4.10. The main characteristic peaks of extracted gibberellic acid from the local isolate of *R. solanacearum* were 3449cm^{-1}, 2985cm^{-1}, and 1720cm^{-1}. The peak at 3449cm^{-1} is attributed to the O-H of the H bond, while the peak at

2985cm^{-1} was attributed to the CH_2 group. The peak at 1720cm^{-1} can be attributed to the C–O of carboxylic acid (Raghavendra *et al.*, 2013). In the FT-IR spectra (Figure. 4.10), there was no observable difference in the main characteristic absorption bands of GA_3standard and GA_3 extracted from a local isolate of *R.solanacearum* infected soils.

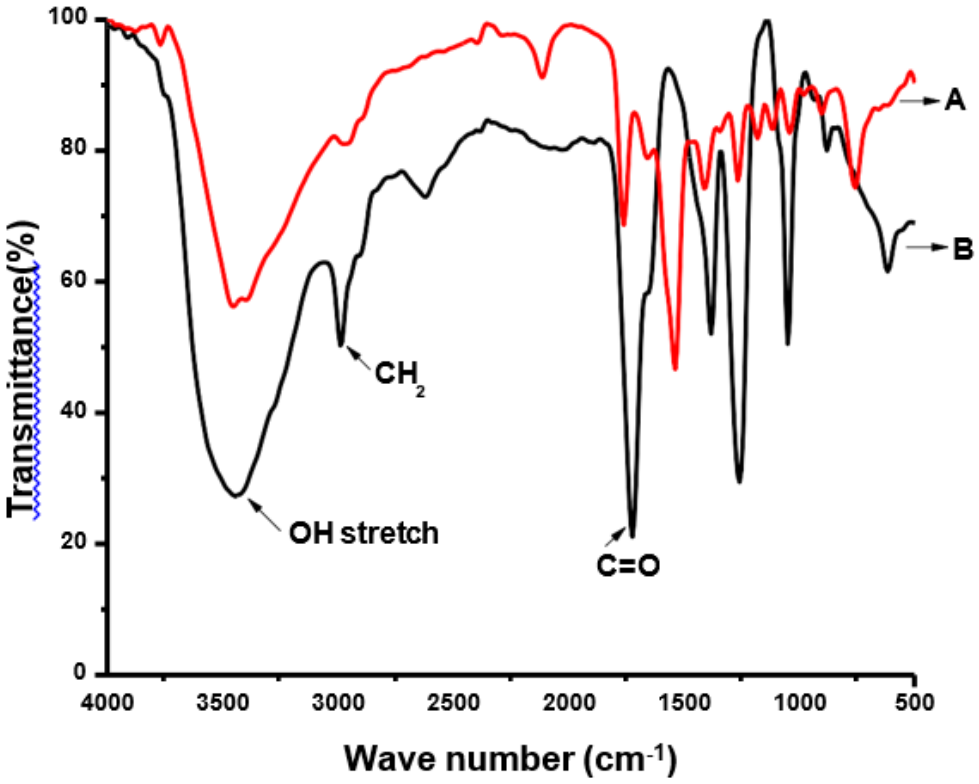

Figure 4.10: FT-IR Spectra of Gibberellic acid (A): Standard gibberellic acid (GA_3), (B):Extracted $GA_3$from a local isolate of R. solanacearum

4.7 Real sample analysis

Detection of the presence of GA_3- mediated *R. solanacearum* using AuNPs was evaluated, and the results are as shown in Figure. 4.11. The colour of the probe changed dramatically

from redto purple, confirming the Bacterial wilt pathogen presence in the infected soils. The increased colour changes corresponded to the broadening of the spectral bandwidth and varied depending on the *Ralstonia* concentration in each tested sample. The distinguishable colour change facilitates the development of a simple sensor for bacterial wilt detection. The intensity of the AuNPs at 520nm becomes weaker with new surface plasmon resonance peaks appearing with infected soils. A colorimetric method for detecting *E. coli* was developed in a similar experiment. AuNPs bind with *E.coli* through electrostatic interaction recognition with different concentrations of bacteria followed by a colour change from red to blue (Raj *et al.*, 2015).

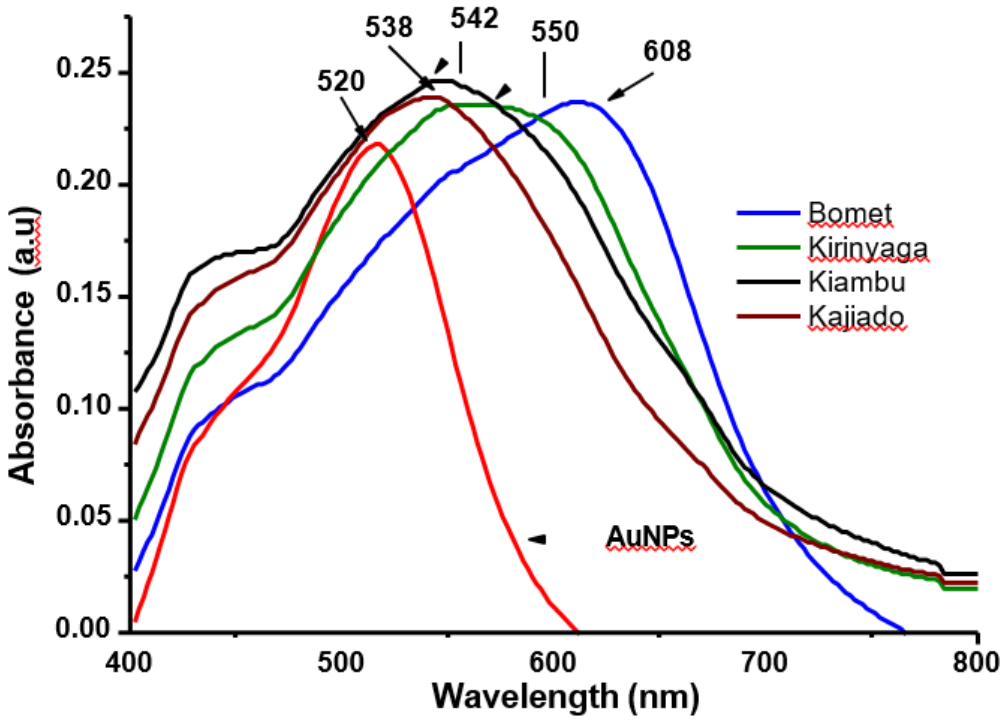

Figure 4.11: U.V.–vis spectra obtained from adding *Bacterial wilt infected soils into AuNPs solution*

A redshift of the plasmon peak with an accompanying broadening of the spectra occurs in a concentration-dependent manner. The highest absorbance with a respectively corresponding broadening of the spectra was observed on the soils from Kiambu county (0.157), followed by Kajiado (0.189) and Kirinyaga (0.214) and Bomet (0.237) soils. In this study, the shifts in the plasmon peak can be attributed to GA_3-induced bacteria, which caused a change in absorbance by inducing aggregation of AuNPs through electrostatic interaction recognition. The degree of aggregation of the probe is dependent on the levels of GA_3 produced by bacteria. If only a small number of bacteria were present in the reaction system, the aggregation would not have proceeded significantly due to the limited availability of bacteria that could bridge the AuNPs.

4.8 Greenhouse assay

Response assays to *R. solanacearum* were monitored with 4-week-old acclimatized tomato plants. All wounded plants in all the treatments wilted within 12 d of inoculation. Negative control plants did not wilt. Plants inoculated with a lower concentration of *R.solanacearum* took longer to wilt than plants inoculated with 10^8CFU/ml. Pathogenicity was confirmed by developing symptoms within seven days, followed by re-isolation and identification of the causal organism from diseased plants as described in section 3.6.2 above.

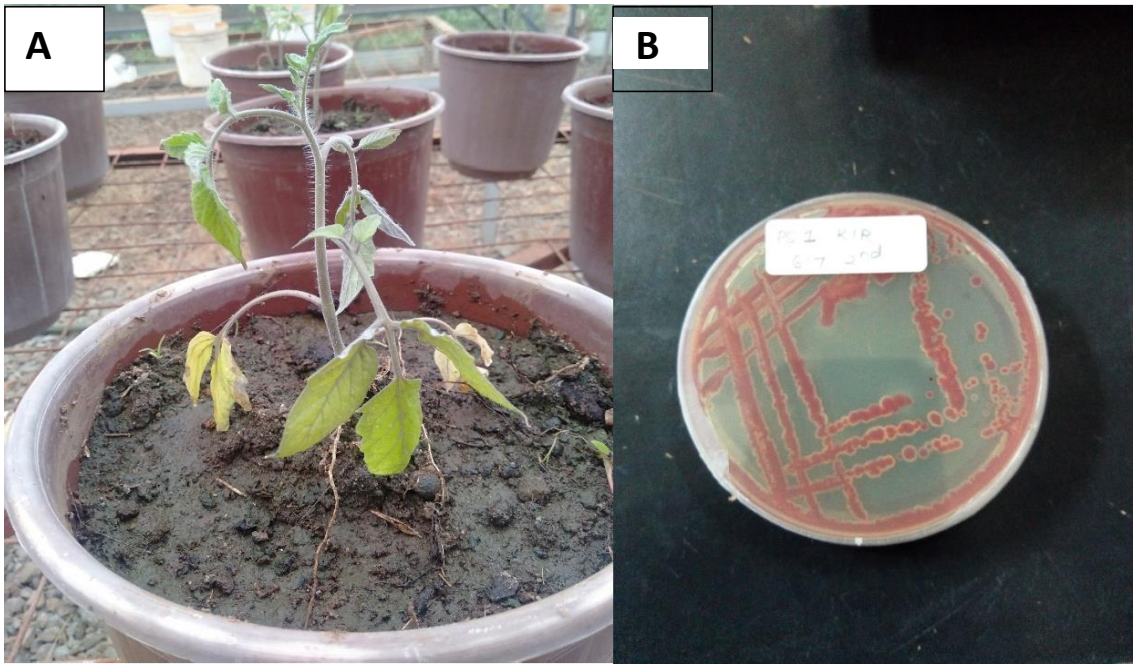

Figure 4.12: A) Wilted tomato plant, 12 days post-inoculation B) Morphological colonies ofbacterial wilt pathogen isolate at 48h of inoculation on CPG media

Re-isolation of bacteria onto CPG media amended with TZC was performed from the vascular tissue of inoculated and non-inoculated control plants. Identification of re-isolated pathogen was carried out morphologically according to Buddenhagen & Kelman,1982. The virulent colonies were identified as irregularly-round, fluidal and white in colour colonies which developed light pink centres (Fig 4.12). The weakly virulent colonies form small butyrous colonies with adistinct dark red colour.

CHAPTER FIVE

SUMMARY, CONCLUSIONS AND RECOMMENDATIONS

5.1 Summary

This study reports a simple colorimetric probe based on gold nanoparticles (AuNPs) for detecting GA_3 produced by *Ralstonia solanacearum.* Gibberellic acid is an essential secondarymetabolite produced by *R.solanacearum*. In this regard, the present study has been devoted to investigating the effect of gibberellic acid-mediated *R.solanacearum* to detect bacterial wilt in tomato production. The study included developing a gold nanoparticle-based diagnostic probe, isolation and quantification of gibberellic acid from *R.solanacearum* cultures, and performance testing of developed probe in-vitro to determine its efficacy. The results illustrated the use ofSPR wavelength-shift sensing and visual colour change to detect GA-mediated *R. solanacearum*. This study also involved soil and plant sampling of infected tomato plants from Kajiado, Kirinyaga, Kiambu, and Bomet counties in Kenya. These areas are documented as bacterial wilt endemic areas in Kenya.

5.2 Conclusion

The thesis presents the development and validation of a simple gold nanoparticle-based colorimetric probe to detect bacterial wilt in Kenya. A gold nanoparticle based colorimetric probe was developed using the citrate reduction method. The gold nanoparticles were characterized based on optical and morphological characteristics in order to determine to their properties. They were stored in a dark colored bottle up to a month. Reaction conditions during synthesis were also optimized to determine ideal conditions for the development of gold nanoparticles. The developed sensor showed a red shift with broadening of the spectrum with different concentrations of synthetic GA_3 standard. A colorimetric method was used to further develop a method to detect GA_3 mediated *R.solanacearum* using unmodified AuNPs. This approach relies on aggregation

of AuNPs which were induced by GA_3 causing color change from red to blue. This assay is based on the distance-dependent optical property of AuNPs and the efficient electrostatic interaction between the AuNPs and GA_3. Our strategy has various advantages including simplicity, convenience and low cost. The high sensitivity gold nanoparticles play a crucial role in designing the pathogen probe with innovative sensing properties for field use. The results demonstrated that gold nanoparticles exhibit excellent optical and surface characteristics that can be manipulated to detect target molecules. The probe willplay a vital role in the early detection of *R. solanacearum* pathogen from other various sources such as water and seed. The probe will also assist farmers in identifying endemic and non- endemic areas before crop establishment to avoid establishing crops in such areas. This will improve tomato production volumes under both protected environments such as greenhouses as well as under field conditions. The method presented in this work demonstrated the possibility of having alternative ways to complement the conventional methods for detecting bacterial wilt, which often include large sample volumes, extensive sample preparation steps, and the use of expensive instrumentation. The developed probe is a promising tool for detecting *R.solanacearum* in low resource settings, especially smallholder farming systems. In the light of the urgent need to develop new, more efficient, accessible, economically viable, and environmentally friendly techniques for detecting destructive plant pathogens, current research developments in the field of nanotechnology and the efficient immobilization of signaling reagents onto nanofibers offer promising solutions. Nanomaterials, such as electro spun nanofibers, offer an alternative method of incorporating active chemical groups in order to fabricate cheap and efficient probes.

5.3 Recommendations

This work has demonstrated how diagnostic probes can be easily fabricated by functionalizing AuNPs to develop selective and sensitive colorimetric probes for detecting target molecules. Future research should also be geared towards hosting the developed colorimetric probe in suitable material to improve the probe's handling and efficacy. Future efforts should be focused on the development of a strip type detection

kit. This product would be highly applicable to pathogen detection hence reducing the cost of analytical procedures. Undoubtedly, great efforts are needed to promote AuNP-based optical approaches from proof-of-concept research to commercially available analytical tools. Au NP-based optical diagnostic has a great future perspective in the early detection of diseases.

REFERENCES

Abdul, H., Tahir, H. A. S., Gu, Q., Wu, H., Raza, W., Safdar, A., Huang, Z., ... & Gao, X. (2017). Effect of volatile compounds produced by Ralstonia solanacearum on plant growth promoting and systemic resistance inducing potential of Bacillus volatiles. *BMC plant biology*, *17*(1), 1-16.

Ahmad, A., Senapati, S., Khan, M. I., Kumar, R., & Sastry, M. (2003). Extracellular biosynthesis of monodisperse gold nanoparticles by a novel extremophilic actinomycete, Thermomonospora sp. *Langmuir*, *19*(8), 3550-3553.

Ahmed, A., Rushworth, J. V., Hirst, N. A., & Millner, P. A. (2014). Biosensors for whole-cell bacterial detection. *Clinical microbiology reviews*, *27*(3), 631-646.

Alex, S., & Tiwari, A. (2015). Functionalized gold nanoparticles: Synthesis, properties and applications-A review. *Journal of Nanoscience and Nanotechnology*, *15*(3), 1869–1894.

Aloyce, A., Ndakidemi, P. A., & Mbega, E. R. (2017). Identification and management challenges associated with Ralstonia solanacearum (Smith), causal agent of bacterial wilt disease of tomato in Sub-Saharan Africa. *Pakistan Journal of Biological Sciences*, *20*(11), 530–542.

Álvarez, B., López, M. M., & Biosca, E. G. (2008). Survival strategies and pathogenicity of Ralstonia solanacearum phylotype II subjected to prolonged starvation in environmental water microcosms. *Microbiology*, *154*(11), 3590–3598.

Amina, S. J., & Guo, B. (2020). A review on the synthesis and functionalization of gold nanoparticles as a drug delivery vehicle. *International Journal of Nanomedicine*, *15*, 9823–9857.

Anang, B. T., Zulkarnain, Z. A., & Yusif, S. (2013). Production Constraints and Measures

toEnhance the Competitiveness of the Tomato Industry in Wenchi Municipal District of Ghana, *3*(4), 824–838.

Anastacia, M. A. O., Thomas, K. K., & Hilda, W. N. (2011). Evaluation of tomato (Lycopersicon esculentum L .) variety tolerance to foliar diseases at Kenya Agricultural Research Institute Centre-Kitale in North west Kenya, *5*(11), 676–681.

Andres, R., Santhanam, V., Ronald, A., & Venugopal, S. (2008). Metal Nanoparticles. *Dekker Encyclopedia of Nanoscience and Nanotechnology, Second Edition - Six Volume Set (PrintVersion)*, 2079–2090.

Bajaj, M., Pandey, S. K., Wangoo, N., & Sharma, R. K. (2018). Peptide Functionalized Metallic Nanoconstructs: Synthesis, Structural Characterization, and Antimicrobial Evaluation. *ACS Biomaterials Science and Engineering*, *4*(2), 739–747.

Bast, N. G., Comenge, J., & Puntes, V. (2011). Kinetically Controlled Seeded Growth Synthesis of Citrate-Stabilized Gold Nanoparticles of up to 200 nm : Size Focusing versus Ostwald Ripening, 11098–11105.

Bertolini, E., & Olmos, A. (2004). Innovative tools for detection of plant pathogenic viruses andbacteria. *International Microbology*, *6*(January), 233–243.

Bhalla, K., Singh, S. B., & Agarwal, R. (2010). Quantitative determination of gibberellins by high performance liquid chromatography from various gibberellins producing Fusarium strains. *Environmental Monitoring and Assessment*, *167*(1–4), 515–520.

Bindhu, M. R., & Umadevi, M. (2014). Antibacterial activities of green synthesized gold nanoparticles. *Materials Letters*, *120*, 122–125.

Bogireddy, N. K. R., Pal, U., Gomez, L. M., & Agarwal, V. (2018). Size controlled green synthesis of gold nanoparticles using Coffea arabica seed extract and their catalytic performance in 4-nitrophenol reduction. *RSC Advances*, *8*(44), 24819–24826.

Bottini, R., Cassán, F., & Piccoli, P. (2004). Gibberellin production by bacteria and its involvement in plant growth promotion and yield increase. *Applied Microbiology andBiotechnology*, *65*(5), 497–503.

Brust, M., Walker, M., Bethell, D., Schiffrin, D. J., & Whyman, R. (2000). Synthesis of Thiol-derivatised Gold Nanoparticles in, 801–802.

Buddenhagen, I., & Kelman,Arthur. (1982). *Biological and Physiological Aspects of BacterialWilt caused by Pseudomonas solanacearum* (Vol. 17).

Champoiseau, P. G., & Momol, T. M. (2008). Bacterial wilt of tomato. *Ralstonia solanacearum*, *12*.

Champoiseau, P. G., Jones, J. B., & Allen, C. (2009). Ralstonia solanacearum race 3 biovar 2 causes tropical losses and temperate anxieties. *Plant Health Progress*, *10*(1), 35.

Chen, Yijun, Wu, X., Lv, L., Li, F., Liu, Z., Kong, Q., & Li, C. (2017). Enhancing reducingability of α-zein by fibrillation for synthesis of Au nanocrystals with continuous flow catalysis. *Journal of Colloid and Interface Science*, *491*, 37–43.

Chen, Ying, Gu, X., Nie, C. G., Jiang, Z. Y., Xie, Z. X., & Lin, C. J. (2005). Shape controlled growth of gold nanoparticles by a solution synthesis. *Chemical Communications*, *1*(33),4181–4183.

Chen, Z., Wang, Z., Chen, J., Wang, S., & Huang, X. (2012). Sensitive and selective

detection ofglutathione based on resonance light scattering using sensitive gold nanoparticles as colorimetric probes. *Analyst*, *137*(13), 3132–3137.

Chitarra, L. G., & Van Den Bulk, R. W. (2003). The application of flow cytometry and fluorescent probe technology for detection and assessment of viability of plant pathogenic bacteria. *European Journal of Plant Pathology*, *109*(5), 407–417.

Choudhary, O. P. (2017). Scanning Electron Microscope : Advantages and Disadvantages in Imaging Components, *6*(5), 1877–1882.

Choudhary, P., Angad, G., Veterinary, D., Choudhary, O. P., & Husbandry, A. (2018). Uses of Transmission Electron Microscope in Microscopy and its Advantages and Disadvantages, *Life Sciences Leaflets*, *85*, 8-to.

Chun Zeng, H. (2007). Ostwald Ripening: A Synthetic Approach for Hollow Nanomaterials, *Current Nanoscience*, *3*(2), 177-181.

Clarke, A. J ., Bailey,J.E. (1973). Nature Publishing Group. *Nat. Phys. Sci.*, *241*, 20

Dalsing, B. L., & Allena, C. (2014). Nitrate assimilation contributes to Ralstonia solanacearum root attachment, stem colonization, and virulence. *Journal of Bacteriology*, *196*(5), 949–960.

de la Rica, R., Aili, D., & Stevens, M. M. (2012). Enzyme-responsive nanoparticles for drug release and diagnostics. *Advanced Drug Delivery Reviews*, *64*(11), 967–978.

Denny, T. (2015). Involvement of Bacterial Polysaccharides in Plant Pathogenesis, . *Annual review of phytopathology*, *33*(1), 173-197.

Dong, J., Carpinone, P. L., Pyrgiotakis, G., Demokritou, P., & Moudgil, B. M. (2020). Synthesis of precision gold nanoparticles using Turkevich method. *KONA*

Powder and Particle Journal, *37*(August), 224–232.

Esther, J., & Sridevi, V. (2017). Synthesis and characterization of chitosan-stabilized gold nanoparticles through a facile and green approach. *Gold Bulletin*, *50*(1).

Evanoff, D. D., & Chumanov, G. (2005). Synthesis and optical properties of silver nanoparticlesand arrays. *ChemPhysChem*, *6*(7), 1221–1231.

Faramarzi, M. A., & Forootanfar, H. (2011). Biosynthesis and characterization of gold nanoparticles produced by laccase from Paraconiothyrium variabile. *Colloids and SurfacesB: Biointerfaces*, *87*(1), 23–27.

Fegan, M., Prior, P., Allen, C., & Hayward, a. C. (2005). How complex is the" Ralstonia solanacearum species complex"? *Bacterial Wilt Disease and the Ralstonia Solanacearum Species Complex*, (February), 449–461. Retrieved from http://www.cabdirect.org/abstracts/20053172646.

Flores-Cruz, Z., & Allen, C. (2011). Necessity of OxyR for the hydrogen peroxide stress response and full virulence in Ralstonia solanacearum. *Applied and Environmental Microbiology*, *77*(18), 6426–6432.

Food, W. (2018). *World food and agriculture*.

Ganaie, S. U., Abbasi, T., Anuradha, J., & Abbasi, S. A. (2014). Biomimetic synthesis of silver nanoparticles using the amphibious weed ipomoea and their application in pollution control.*Journal of King Saud University - Science*, *26*(3), 222–229.

Gatahi, D. M., Wanyika, H. N., & Mumokavoo, A. (2017). Enhancement of bacterial wilt resistance and rhizosphere health in tomato using bionanocomposites, *3*(2), 129–144.

Gavamukulya, Y., Maina, E. N., Meroka, A. M., Madivoli, E. S., El-Shemy, H. A.,

Wamunyokoli, F., & Magoma, G. (2020). Green Synthesis and Characterization of Highly Stable Silver Nanoparticles from Ethanolic Extracts of Fruits of Annona muricata. *Journal of Inorganic and Organometallic Polymers and Materials*, *30*(4), 1231–1242.

Geng, X., & Grove, T. Z. (2015). Repeat protein mediated synthesis of gold nanoparticles: Effect of protein shape on the morphological and optical properties. *RSC Advances*, *5*(3), 2062– 2069.

Gijsegem, F. Van, Genin, S., & Boucher, C. (1993). Conservation of secretion pathways for pathogenicity determinants of plant and animal bacteria, *1*(5), 175–180.

Gomi, K., & Matsuoka, M. (2003). Gibberellin signalling pathway. *Current Opinion in PlantBiology*, *6*(5), 489–493.

Gommes, C. J. (2019). Ostwald ripening of confined nanoparticles: Chemomechanical couplingin nanopores. *Nanoscale*, *11*(15), 7386–7393.

Guieu, V., Ravelet, C., Perrier, S., Zhu, Z., Cayez, S., & Peyrin, E. (2011). Analytica Chimica Acta Aptamer enzymatic cleavage protection assay for the gold nanoparticle-based colorimetric sensing of small molecules, *706*, 349–353.

Haiss, W., Thanh, N. T. K., Aveyard, J., & Fernig, D. G. (2007). Determination of size and concentration of gold nanoparticles from UV-Vis spectra. *Analytical Chemistry*, *79*(11),4215–4221.

HCD. (2019). 2017-2018 Validated Horticulture Data Report. Retrieved from http://horticulture.agricultureauthority.go.ke/index.php/statistics/reports

Hennessy, J., Wilson, J. K., Stead, D. E., Hutton, S., & Directive, H. (1996). solanacearum inpotato tuber extracts. *EPPO Bull*, *678*, 663–678.

Herizchi, R., Abbasi, E., Milani, M., & Akbarzadeh, A. (2016). Current methods for synthesis of gold nanoparticles. *Artificial Cells, Nanomedicine and*

Biotechnology, *44*(2), 596–602.

Ireri, D. F., Murungi, L. K., Ngeno, D. C., & Mbaka, J. (2018). Farmer knowledge of bacterial wilt and root-knot nematodes and practices to control the pathogens in high tunnel tomato production in the tropics. *International Journal of Vegetable Science*, *00*(00), 1–13.

Jongjinakool, S., Palasak, K., Bousod, N., & Teepoo, S. (2014). Gold nanoparticles-based colorimetric sensor for cysteine detection. *Energy Procedia*, *56*(C), 10–18.

Karadeniz, A., Topcuoğlu, Ş. F., & Inan, S. (2006). Auxin, gibberellin, cytokinin and abscisicacid production in some bacteria. *World Journal of Microbiology and Biotechnology*, *22*(10), 1061–1064.

Khalid, A., Arshad, M., & Zahir, Z. A. (2004). Screening plant growth-promoting rhizobacteria for improving growth and yield of wheat. *Journal of Applied Microbiology*, *96*(3), 473–480.

Khodashenas, B., Ardjmand, M., Rad, A. S., & Esfahani, M. R. (2021). Gelatin-coated gold nanoparticles as an effective pH-sensitive methotrexate drug delivery system for breastcancer treatment. *Materials Today Chemistry*, *20*, 100474.

Kumar, S., Gandhi, K. S., & Kumar, R. (2007). Modeling of formation of gold nanoparticles by citrate method. *Industrial and Engineering Chemistry Research*, *46*(10), 3128–3136.

Lee, J., Kim, H. Y., Zhou, H., Hwang, S., Koh, K., Han, D. W., & Lee, J. (2011). Green synthesis of phytochemical-stabilized Au nanoparticles under ambient conditions and their biocompatibility and antioxidative activity. *Journal of Materials Chemistry*, *21*(35), 13316–13326.

Lee, K. X., Shameli, K., Yew, Y. P., Teow, S. Y., Jahangirian, H., Rafiee-Moghaddam,

R., & Webster, T. J. (2020). Recent developments in the facile bio-synthesis of gold nanoparticles (AuNPs) and their biomedical applications. *International Journal of Nanomedicine*, *15*, 275–300.

Li, X., Xu, H., Chen, Z. S., & Chen, G. (2011). Biosynthesis of nanoparticles by microorganisms and their applications. *Journal of Nanomaterials*, *2011(8), 1-16*.

Lin, S. Y., Tsai, Y. T., Chen, C. C., Lin, C. M., & Chen, C. H. (2004). Two-step functionalization of neutral and positively charged thiols onto citrate-stabilized Aunanoparticles. *Journal of Physical Chemistry B*, *108*(7), 2134–2139.

Lowe-Power, T. M., Jacobs, J. M., Ailloud, F., Fochs, B., Prior, P., & Allen, C. (2016). Degradation of the Plant Defense Signal Salicylic Acid Protects. *MBio*, *7*(3), 1–12.

M.C. Daniel, D. A. (2004). Gold nanoparticles: assembly, supramolecularchemistry, quantum- size-related properties, and applications toward. *Chem. Rev.*, *104*, 293– 346.

Mansfield, J., Genin, S., Magori, S., Citovsky, V., Sriariyanum, M., Ronald, P., … Tolosan, F.-C. (2012). Top 10 plant pathogenic bacteria in molecular plant pathology. *Mol. Plant Pathol. 13*, *13*, 614–629.

Martínez-Morales, L. J., Soto-Urzúa, L., Baca, B. E., & Sánchez-Ahédo, J. A. (2003). Indole-3-butyric acid (IBA) production in culture medium by wild strain Azospirillum brasilense. *FEMS Microbiology Letters*, *228*(2), 167–173.

Martinez-Toledo, M. V., de la Rubia, T., Moreno, J., & Gonzalez-Lopez, J. (1988). Root exudates of Zea mays and production of auxins, gibberellins and cytokinins by Azotobacter chroococcum. *Plant and Soil*, *110*(1), 149–152.

Milling, A., Babujee, L., & Allen, C. (2011). Ralstonia solanacearum extracellular polysaccharide is a specific elicitor of defense responses in wilt-resistant tomato plants. *PLoS ONE*, *6*(1).

Monteiro, F., Genin, S., van Dijk, I., & Valls, M. (2012). A luminescent reporter evidences active expression of Ralstonia solanacearum type III secretion system genes throughout plant infection. *Microbiology (United Kingdom)*, *158*(8), 2107–2116.

Muthoni, J., Shimelis, H., & Melis, R. (2012). Management of Bacterial Wilt [Rhalstonia solanacearum Yabuuchi et al., 1995] of Potatoes: Opportunity for Host Resistance in Kenya. *Journal of Agricultural Science*, *4*(9), 64–78.

Mwangi, T. M., Ndirangu, S. N., & Isaboke, H. N. (2020). Technical efficiency in tomato production among smallholder farmers in Kirinyaga County , Kenya, *16*(5), 667–677.

N'Guessan, C. A., Abo, K., Fondio, L., Chiroleu, F., Lebeau, A., Poussier, S., … Koné, D. (2012). So Near and Yet so Far: The Specific Case of *Ralstonia solanacearum* Populations from Côte d'Ivoire in Africa. *Phytopathology*, *102*(8), 733–740.

Niemeyer, C. M. (2002). The developments of semisynthetic DNA-protein conjugates. *Trends inBiotechnology*, *20*(9), 395–401.

Niidome, Y., Nishioka, K., Kawasaki, H., & Yamada, S. (2003). Rapid synthesis of gold nanorods by the combination of chemical reduction and photoirradiation processes; morphological changes depending on the growing processes. *Chemical Communications*,*3*(18), 2376–2377.

Ongeri, B. O. (2014). Small Scale Horticultural farming along the Kenyan Highways and Local economic development: Exploring the effect of factor prices.

International Review of Research in Emerging Markets and the Global Economy (IRREM) An Online InternationalResearch Journal, *1*(3), 2311–3200.

Ovais, M., Khalil, A. T., Islam, N. U., Ahmad, I., Ayaz, M., Saravanan, M., …& Mukherjee, S.(2018). Role of plant phytochemicals and microbial enzymes in biosynthesis of metallic nanoparticles. *Applied Microbiology and Biotechnology*, *102*(16), 6799–6814.

Pang, C., Jung, J. Y., Lee, J. W., & Kang, Y. T. (2012). Thermal conductivity measurement of methanol-based nanofluids with Al 2O 3 and SiO 2 nanoparticles. *International Journal ofHeat and Mass Transfer*, *55*(21–22), 5597–5602.

Paret, M. L., Kubota, R., Jenkins, D. M., & Alvarez, A. M. (2010). Survival of *Ralstonia solanacearum* race 4 in drainage water and soil and detection with immunodiagnostic andDNA-based assays. *HortTechnology*, *20*(3), 539–548.

Park, J., & Shumaker-parry, J. S. (2020). Structural Study of Citrate Layers on Gold Nanoparticles: Role of Intermolecular Interactions in Stabilizing Nanoparticles. *J. Am. Chem. Soc.*, *136*, 1907–1921.

Patel, K., Goswami, D., Dhandhukia, P., & Thakker, J. (2015). Techniques to study microbial phytohormones. *Bacterial metabolites in sustainable agroecosystem*, 1-27.

Peeters, N., Guidot, A., Vailleau, F., & Valls, M. (2013). *Ralstonia solanacearum*, a widespread bacterial plant pathogen in the post-genomic era. *Molecular Plant Pathology*, *14*(7), 651–662.

Philip, D. (2010). Rapid green synthesis of spherical gold nanoparticles using Mangifera indica leaf. *Spectrochimica Acta - Part A: Molecular and Biomolecular*

Spectroscopy, *77*(4), 807–810.

Pienpinijtham, P., Thammacharoen, C., & Ekgasit, S. (2012). Green synthesis of size controllable and uniform gold nanospheres using alkaline degradation intermediates of soluble starch as reducing agent and stabilizer. *Macromolecular Research*, *20*(12), 1281–1288.

Priyadarshini, E., & Pradhan, N. (2017). Gold nanoparticles as efficient sensors in colorimetric detection of toxic metal ions: A review. *Sensors and Actuators, B: Chemical*, *238*, 888–902.

Raghavendra, G. M., Jayaramudu, T., Varaprasad, K., Sadiku, R., Ray, S. S., & Mohana Raju, K. (2013). Cellulose-polymer-Ag nanocomposite fibers for antibacterial fabrics/skin scaffolds. *Carbohydrate Polymers*, *93*(2), 553–560.

Raj, V., Vijayan, A. N., & Joseph, K. (2015). Cysteine capped gold nanoparticles for naked eye detection of E. coli bacteria in UTI patients. *Sensing and Bio-Sensing Research*, *5*, 33–36.

Ramasamy, S., & Ravishankar, M. (2018). Integrated pest management strategies for tomato under protected structures. In *Sustainable Management of Arthropod Pests of Tomato* (pp. 313-322). New York: Academic Press.

Rashid, R., Murtaza, G., & Zahra, A. (2014). Gold nanoparticles: synthesis and applications in drug delivery. *Tropical journal of pharmaceutical research*, *13*(7), 1169-1177.

Rosi, N. L., & Mirkin, C. A. (2005). Nanostructures in biodiagnostics BT - Chemical reviews, *105*(4), 1547–1562.

Saha, S. K., Roy, P., Mondal, M. K., Roy, D., Gayen, P., Chowdhury, P., & Babu, S. P. S. (2017). Development of chitosan based gold nanomaterial as an efficient

antifilarial agent: A mechanistic approach. *Carbohydrate Polymers*, *157*, 1666–1676.

Sandhu, R., Singh, N., & Dhankhar, J. (2018). Dynamic light scattering (DLS) technique , principle , theoretical considerations and applications, *Nanotechnol. Biochem. Tech. Assess. Qual. Saf. Milk Milk Prod*, 135-137.

Sciences, P., Sabir, S., Asghar, H. N., Kashif, S. U. R., Khan, M. Y., Akhtar, M. J., & Sciences, A. (2013). Synergistic effect of plant growth promoting rhizobacteria and kinetin on maize. *J. Anim. Plant Sci.*, *23*(6), 1750–1755.

Senapati, S., Ahmad, A., Khan, M. I., Sastry, M., & Kumar, R. (2005). Extracellular biosynthesis of bimetallic Au-Ag alloy nanoparticles. *Small*, *1*(5), 517–520.

Sharma, S., Sharma, A., & Kaur, M. (2018). Growth promoting rhizobacteria Extraction and evaluation of gibberellic acid from Pseudomonas sp.: Plant growth promoting rhizobacteria. *J. Pharmacogn. Phytochem*, *7*, 2790-2795.

Shoukry, A. A., El-Sebaay, H. H., & El-Ghomary, A. E. (2018). Assessment of Indole Acetic Acid Production from Rhizobium leguminosarum Strains. *Current Science International*,*7*(1), 60–69.

Silpa, D., Rao, P. B., Kumar, G. K., & Ram, M. R. (2018). Studies on Gibberellic Acid Production by Bacillus Licheniformis DS3 Isolated from Banana Field Soils, *4*(5), 1106–1112.

Slistan-Grijalva, A., Herrera-Urbina, R., Rivas-Silva, J. F., Ávalos-Borja, M., Castillón-Barraza, F. F., & Posada-Amarillas, A. (2005). Classical theoretical characterization of the surface plasmon absorption band for silver spherical nanoparticles suspended in water and ethylene glycol. *Physica E: Low-Dimensional Systems and Nanostructures*, *27*(1–2), 104–112.

Song, J. Y., Jang, H. K., & Kim, B. S. (2009). Biological synthesis of gold nanoparticles using Magnolia kobus and Diopyros kaki leaf extracts. *Process Biochemistry*, *44*(10), 1133–1138.

Srivastava, S., Frankamp, B. L., & Rotello, V. M. (2005). Supporting Information ControlledPlasmon Resonance of Gold Nanoparticles Self-Assembled with PAMAM Dendrimers.*Microscopy*, (c), 1–5.

Stevens, K. A., & Jaykus, L. (2014). Bacterial Separation and Concentration from Complex Sample Matrices: A Bacterial Separation and Concentration from Complex Sample Matrices : A Review. *Crit. Rev. Microbiol. 30*, *30*(February), 7–24.

Stewart, M. E., Anderton, C. R., Thompson, L. B., Maria, J., Gray, S. K., Rogers, J. A., & Nuzzo, R. G. (2008). Nanostructured plasmonic sensors. *Chemical Reviews*, *108*(2), 494–521.

Tallury, P., Malhotra, A., Byrne, L. M., & Santra, S. (2010). Nanobioimaging and sensing ofinfectious diseases ☆. *Advanced Drug Delivery Reviews*, *62*(4–5), 424–437.

Teow, Y. H., & Mohammad, A. W. (2019). New generation nanomaterials for water desalination: A review. *Desalination*, (May), 2–17.

Tsegay, M. G., Gebretinsae, H. G., Sackey, J., Maaza, M., & Nuru, Z. Y. (2019). Green synthesis of khat mediated silver nanoparticles for efficient detection of mercury ions. *Materials Today: Proceedings*, *36*(xxxx), 368–373.

Tyagi, H., Kushwaha, A., Kumar, A., & Aslam, M. (2016). A facile pH controlled citrate-based reduction method for gold nanoparticle synthesis at room temperature. *Nanoscale research letters*, *11*(1), 1-11.

Vaseghi, A., Safaie, N., Bakhshinejad, B., Mohsenifar, A., & Sadeghizadeh, M. (2013). Detection of Pseudomonas syringae pathovars by thiol-linked DNA-Gold nanoparticleprobes. *Sensors and Actuators, B: Chemical*, *181*, 644–651.

Verma, H. N., Singh, P., & Chavan, R. M. (2014). Gold nanoparticle: Synthesis and characterization. *Veterinary World*, *7*(2), 72–77.

Vilela, D., González, M. C., & Escarpa, A. (2012). Sensing colorimetric approaches based on gold and silver nanoparticles aggregation: Chemical creativity behind the assay. A review.*Analytica Chimica Acta*, *751*, 24–43.

Yu, J., Xu, D., Guan, H. N., Wang, C., Huang, L. K., & Chi, D. F. (2016). Facile one-step greensynthesis of gold nanoparticles using Citrus maxima aqueous extracts and its catalytic activity. *Materials Letters*, *166*(26), 110–112.

Yuliar, Nion, Y. A., & Toyota, K. (2015). Recent Trends in Control Methods for Bacterial Wilt Diseases Caused by *Ralstonia solanacearum*. *Microbes and Environments*, *00*(0).

Yürekli, F., Yesilada, O., Yürekli, M., & Topcuoglu, S. F. (1999). Plant growth hormone production from olive oil mill and alcohol factory wastewaters by white rot fungi. *WorldJournal of Microbiology and Biotechnology*, *15*(4), 503–505.

Zhao, W., Ali, M. M., Aguirre, S. D., Brook, M. A., & Li, Y. (2008). #Zhao2008.Pdf, *80*(22), 8431–8437.

Zhao, W., Brook, M. A., & Li, Y. (2008). Design of gold nanoparticle-based colorimetric biosensing assays. *ChemBioChem*, *9*(15), 2363–2371.